Our dark matter halo

Milky Way

Dark matter halo

Image credit: ESO/L Calçada

We are here.

Observations of our galaxy tell us:
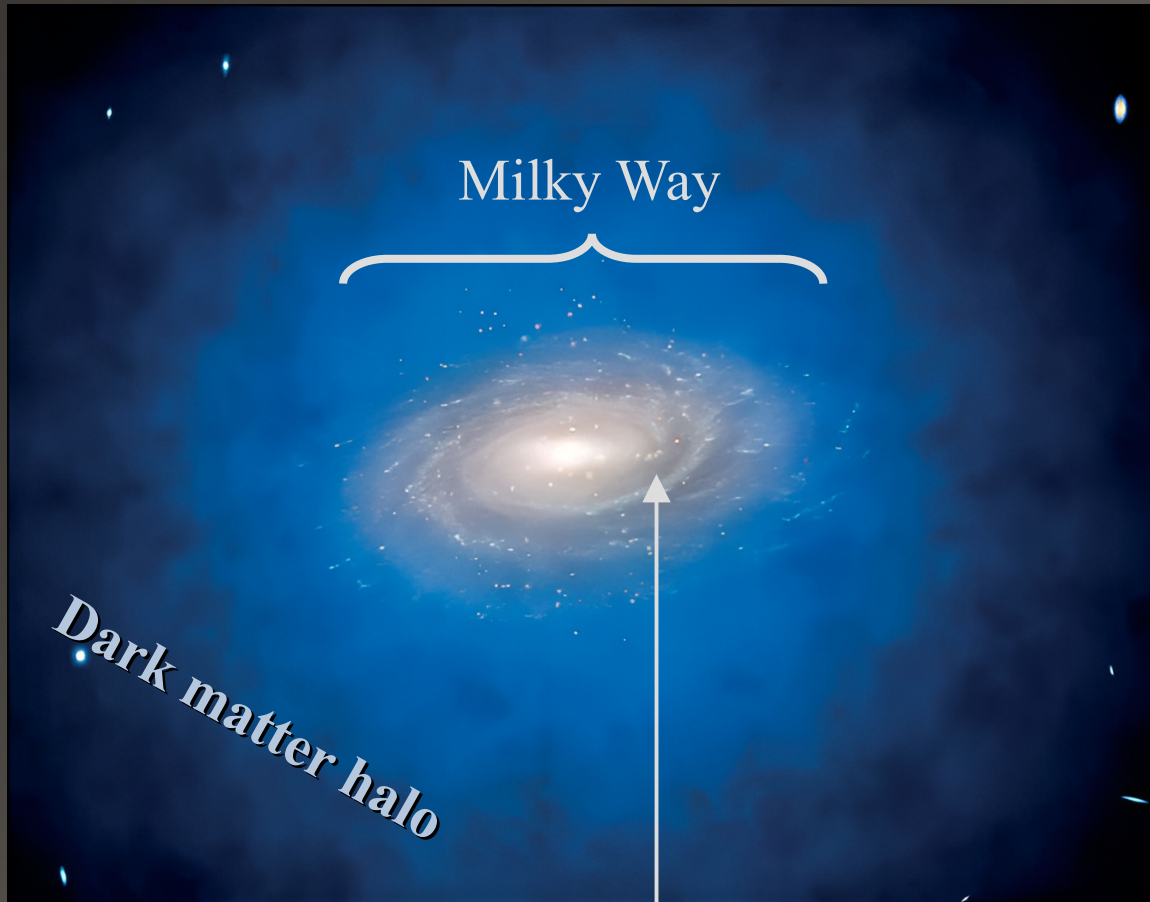
Local dark matter density

$$\rho_{\mathrm{DM}} = 0.4\,\mathrm{GeV/cm^3}$$

Local dark matter velocity

$$\langle v_{\mathrm{DM}} \rangle \approx 300\,\mathrm{km/s}$$

Lighter masses $\rightarrow$ more particles

$$n_{\mathrm{DM}} = \rho_{\mathrm{DM}}/m_{\mathrm{DM}}$$

More particles $\rightarrow$ larger fluxes

$$\phi_{\mathrm{DM}} \sim v_{\mathrm{DM}}\, n_{\mathrm{DM}}$$

Direct detection

χ χ

$\vec{q}$

$|\Psi_i\rangle \longrightarrow \quad\quad\quad \longrightarrow |\Psi_f\rangle$
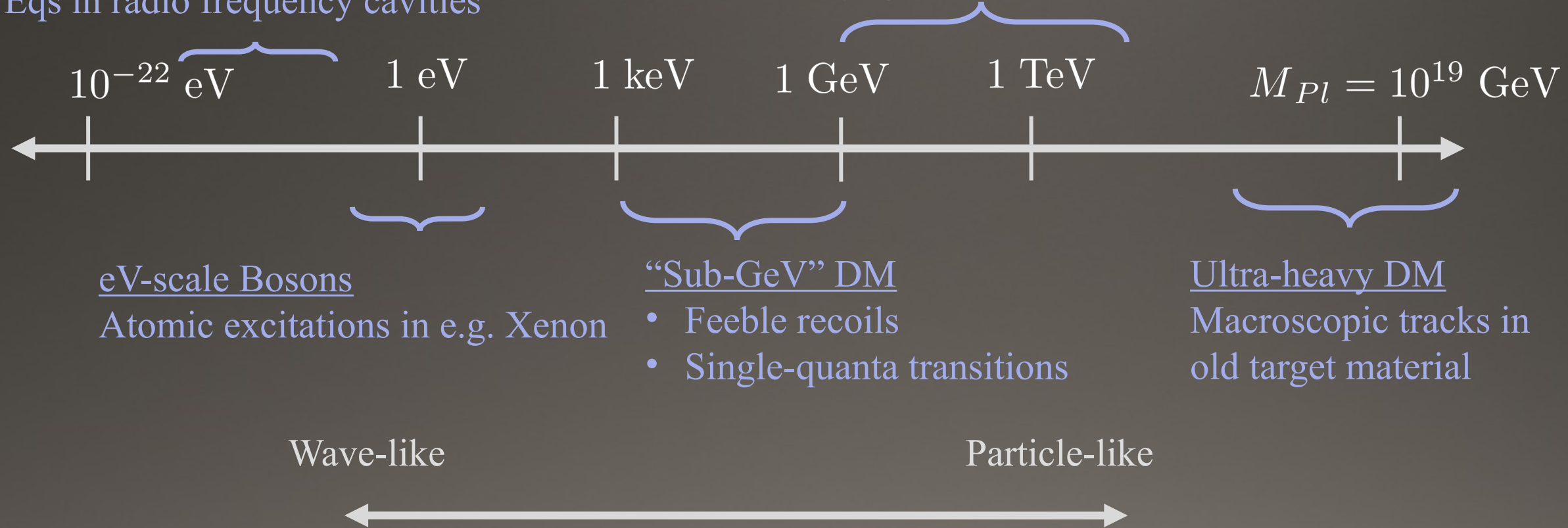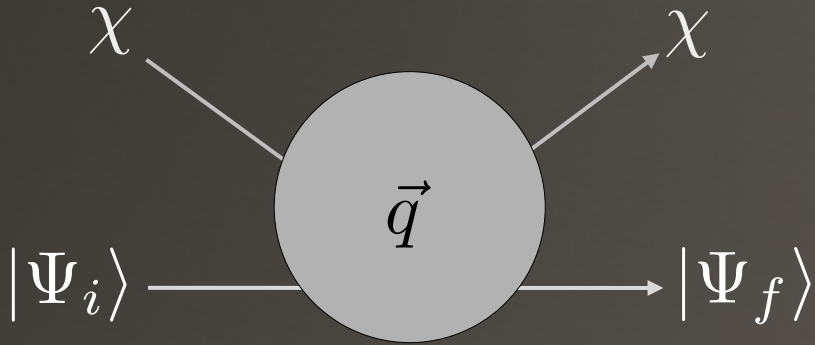
$$\bar{R}_{\text{sig}} \sim \xi \phi_{\text{DM}} \sigma \gtrsim \bar{R}_{\text{bkg}}$$

ξ : Signal generation efficiency

What we need is:
Small threshold energies
Large signal efficiencies
Low backgrounds

$$\sigma_{\text{min}} \gtrsim \bar{R}_{\text{bkg}}/\phi_{\text{DM}}\xi$$

Benchmark gives right DM abundance

$\sigma_{e/n}\,[\text{cm}^2]$

$m_{\chi\text{min}} \sim \Delta E_r/v^2$

Excluded

Freeze-out or Freeze-in

$\phi_{\text{DM}} \sim v_{\text{DM}}\, n_{\text{DM}}$

$m_{\text{DM}}\,[\text{GeV}]$
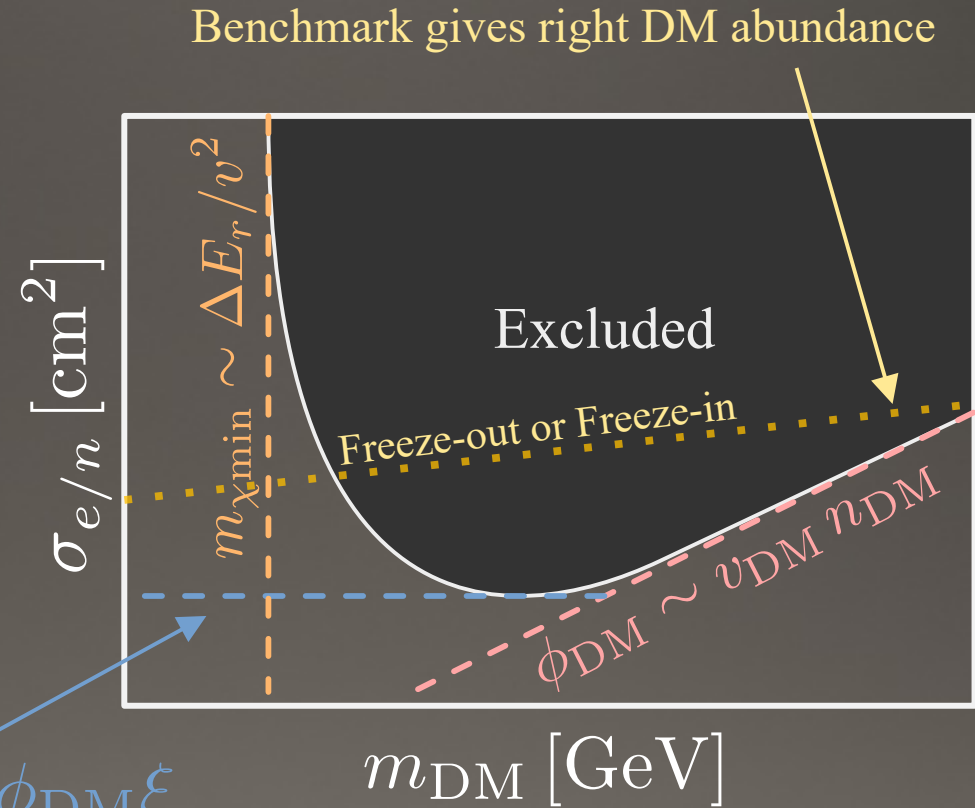
Sub-GeV direct detection

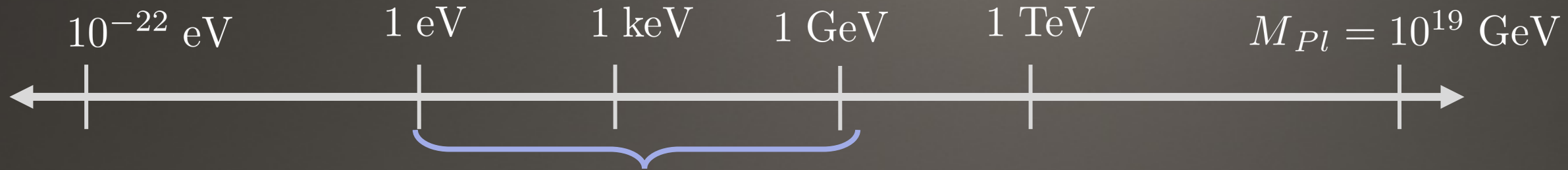$$10^{-22} \text{ eV} \qquad 1 \text{ eV} \qquad 1 \text{ keV} \qquad 1 \text{ GeV} \qquad 1 \text{ TeV} \qquad M_{Pl} = 10^{19} \text{ GeV}$$

eV-scale Bosons & "Sub-GeV" DM
Classically allowed absorption & Inelastic scattering in **molecules** and **nanomaterials**
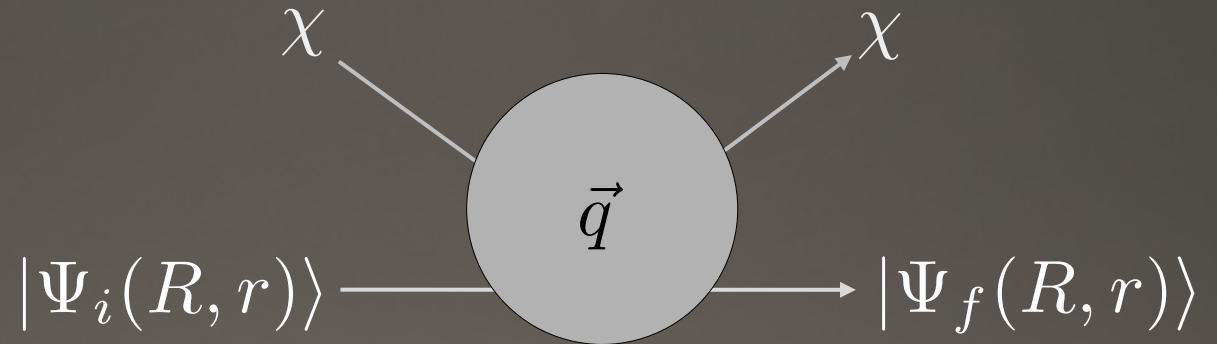
Kinetic energy of the dark matter

$$\Delta E \sim 10^{-6} m_\chi \approx \mathcal{O}(\text{eV}) \left(\frac{\text{m}_\chi}{1 \text{ MeV}} \right)$$

Imparted momentum in *scattering*

$$|q| \sim m_\chi v_\chi \approx \mathcal{O}(\text{keV}) \left(\frac{m_\chi}{1 \text{ MeV}} \right)$$

Imparted energy and momentum in *absorption*

$$|q| \approx 0, \ \Delta E = m_\chi \ (\mathcal{O}(\text{eV}))$$

$\chi \qquad\qquad \chi$

$\vec{q}$

$|\Psi_i(R, r)\rangle \longrightarrow |\Psi_f(R, r)\rangle$

R : Nuclear coordinates
r : Electron coordinates

Interaction Rate

Rate "spectrum" (events in detector)

$$\frac{dR}{d\ln E_r} \sim \int \frac{d^3\vec{q}}{q} \eta(v) |F_{\mathrm{DM}}(q)|^2 |f_{i\to f}(q)|^2$$
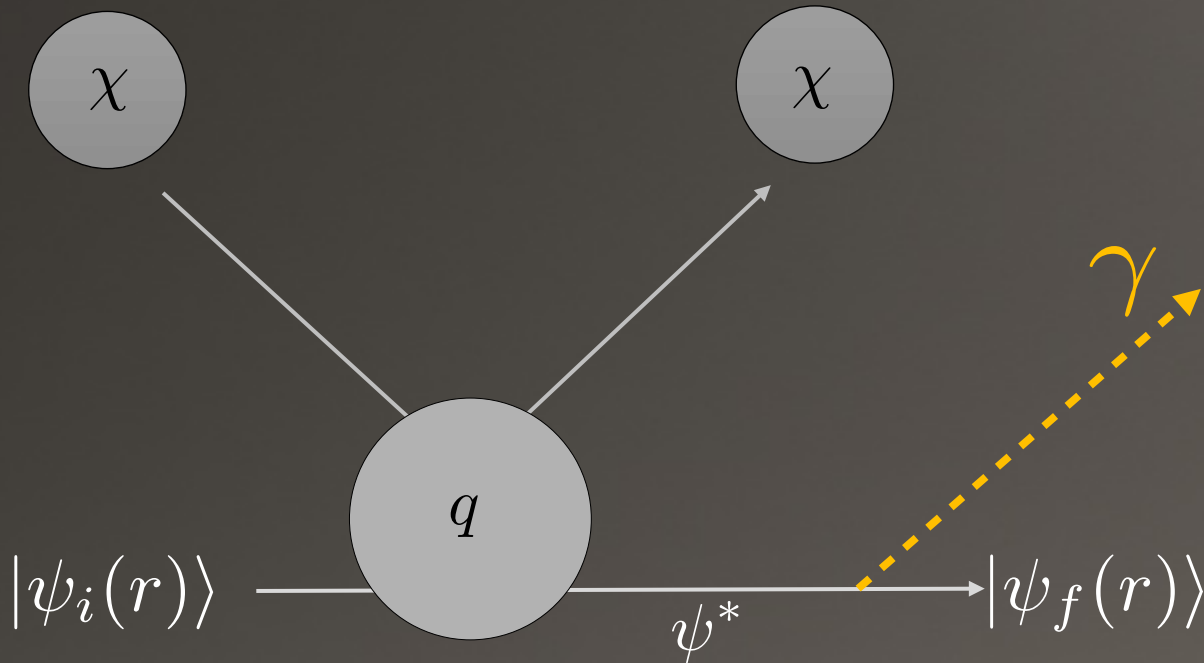
Mean inverse velocity (Astro)

$$\eta(v)$$

Transition form factor (Condensed matter / Chemistry)

$$f_{i\to f}(q) = \langle \Psi_f | e^{i\vec{q}\cdot\vec{r}} | \Psi_i \rangle = \langle \tilde{\Psi}_f(k+q) | \tilde{\Psi}_i(k) \rangle$$

Dark matter form factor (Particle physics)

$$F_{\mathrm{DM}}(q) = \begin{cases} 1 & \text{, Contact interaction} \\ \left(\dfrac{\alpha m_e}{q}\right)^2 & \text{, Long-range interaction} \end{cases}$$

Electron Recoil: Photon Signal

Electron scattering or bosonic absorption leads to an excitation that decays via radiative emission.

A small unit that de-excites by emitting a photon is called a *chromophore*.

Electrons in crystals (exciton generation)

$$|\psi_i\rangle \sim u_v(r)e^{ik\cdot r} \quad |\psi\rangle^* \sim u_c(r)e^{ik\cdot r}$$
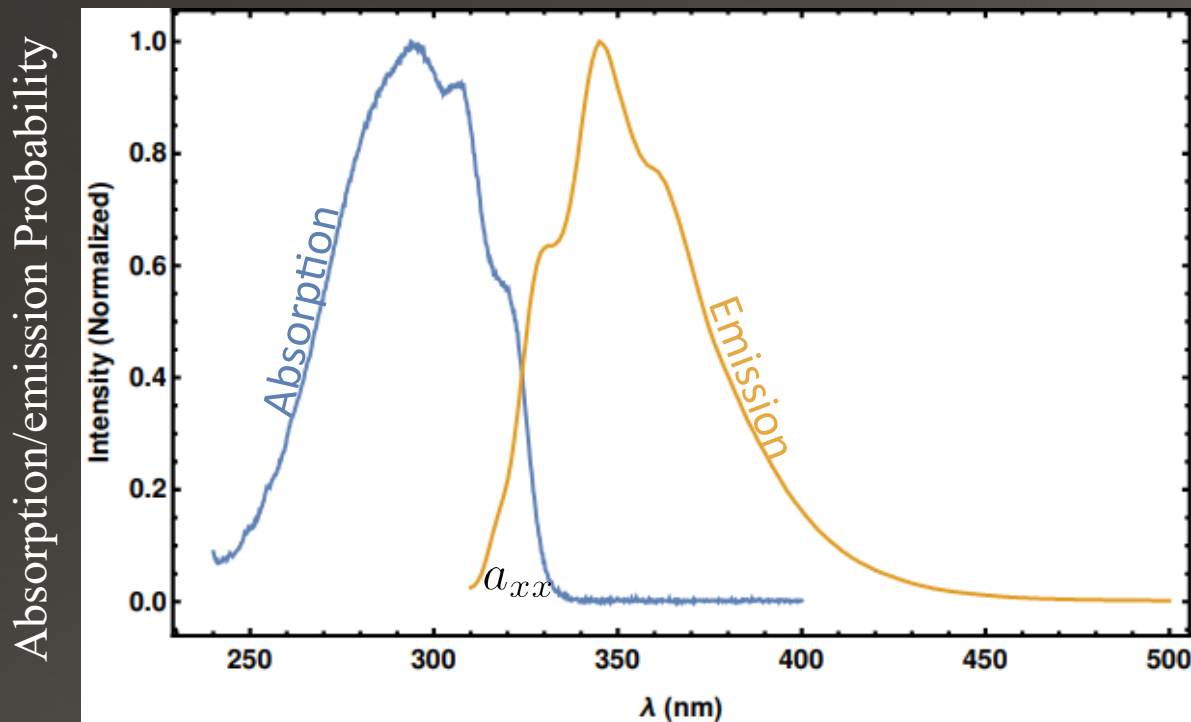
Excite from valence to conduction

Electrons in molecules and atoms

$$|\psi_i\rangle \sim \psi_{\text{lcao}}(r) \quad |\psi\rangle^* \sim \psi_{lcao}^*(r)$$

Excite quantized levels

Fluorescence with DM
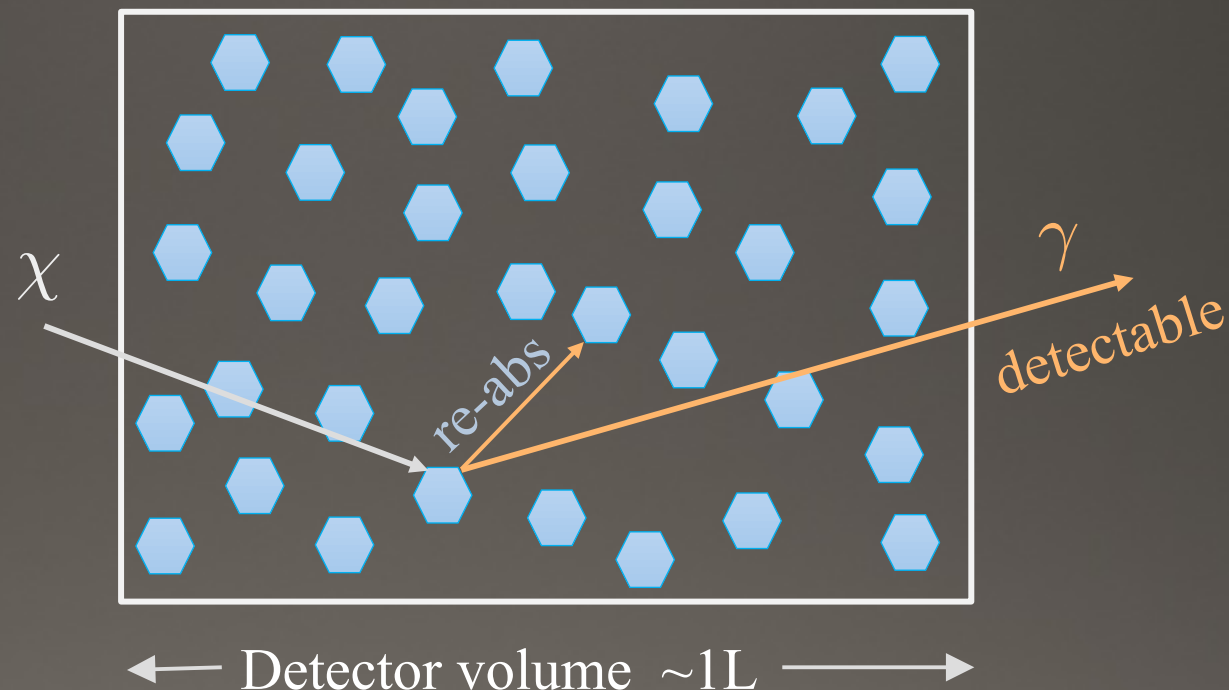
Characteristic fluorescence spectra of chromophores

Decreasing energy (E) →

Large detectable signal efficiencies

Chromophore:

χ
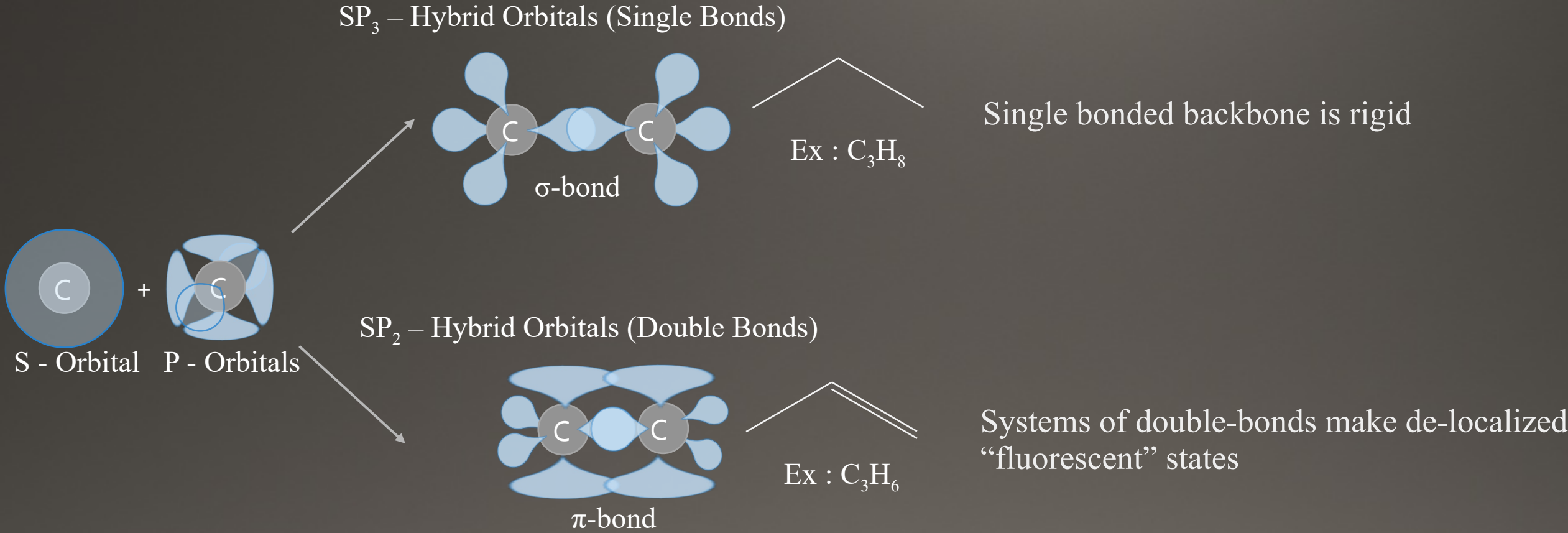
γ

re-abs

detectable

← Detector volume ~1L →

Probability for the photon to free-stream

$$\Phi_{\text{FB}} \sim (1 - a_{xx})$$

Solid molecular crystals: $\Phi_{\text{FB}} \approx 65\%$

Carbon: a natural candidate

SP$_3$ – Hybrid Orbitals (Single Bonds)

σ-bond

Ex : C$_3$H$_8$

Single bonded backbone is rigid

S - Orbital   P - Orbitals

SP$_2$ – Hybrid Orbitals (Double Bonds)

Ex : C$_3$H$_6$

Systems of double-bonds make de-localized "fluorescent" states

π-bond

The de-localized p-orbital networks of carbon-based molecules are natural DM detector candidates

$$q_e \approx 1/a_0 \sim \mathcal{O}(\text{keV})$$

$$|q| \sim m_\chi v_\chi \approx \mathcal{O}(\text{keV}) \left(\frac{m_\chi}{1 \text{ MeV}} \right)$$

A pilot experiment

Problem: describe the interaction between DM (BSM) with molecules (chemistry)

Build the many body wave functions from molecular orbitals

$$\Psi_G = |\psi_2\overline{\psi_2}\psi_1\overline{\psi_1}\psi_{1\prime}\overline{\psi_{1\prime}}|$$

$$\Psi_i^j = \frac{1}{\sqrt{2}}(|\psi_1\overline{\psi_1}...\psi_i\overline{\psi_j}...\psi_N\overline{\psi_N}| - |\psi_1\overline{\psi_1}...\psi_j\overline{\psi_i}...\psi_N\overline{\psi_N}|)$$

Commercially available

Compute the molecular form factors

$$f_i(\mathbf{q}) = \int d^3\mathbf{p}\,\tilde{\psi}_n(\mathbf{p})\tilde{\psi}_{n+i}^\star(\mathbf{p}+\mathbf{q})$$
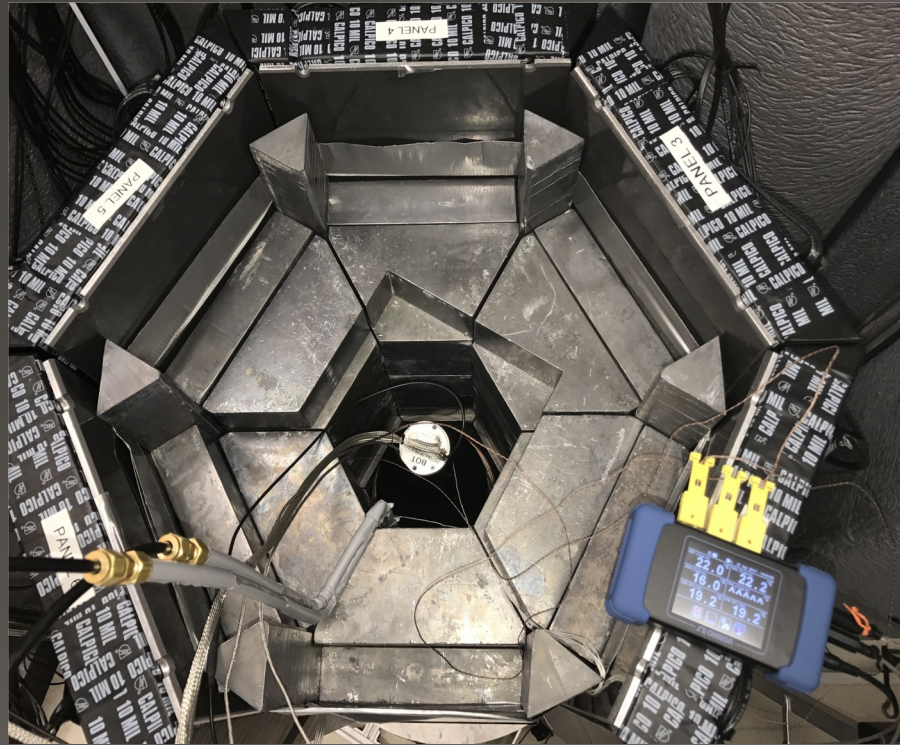
Molecular scintillators are cheap, well characterized, and extremely clean.

Blanco '19: 1912.02822

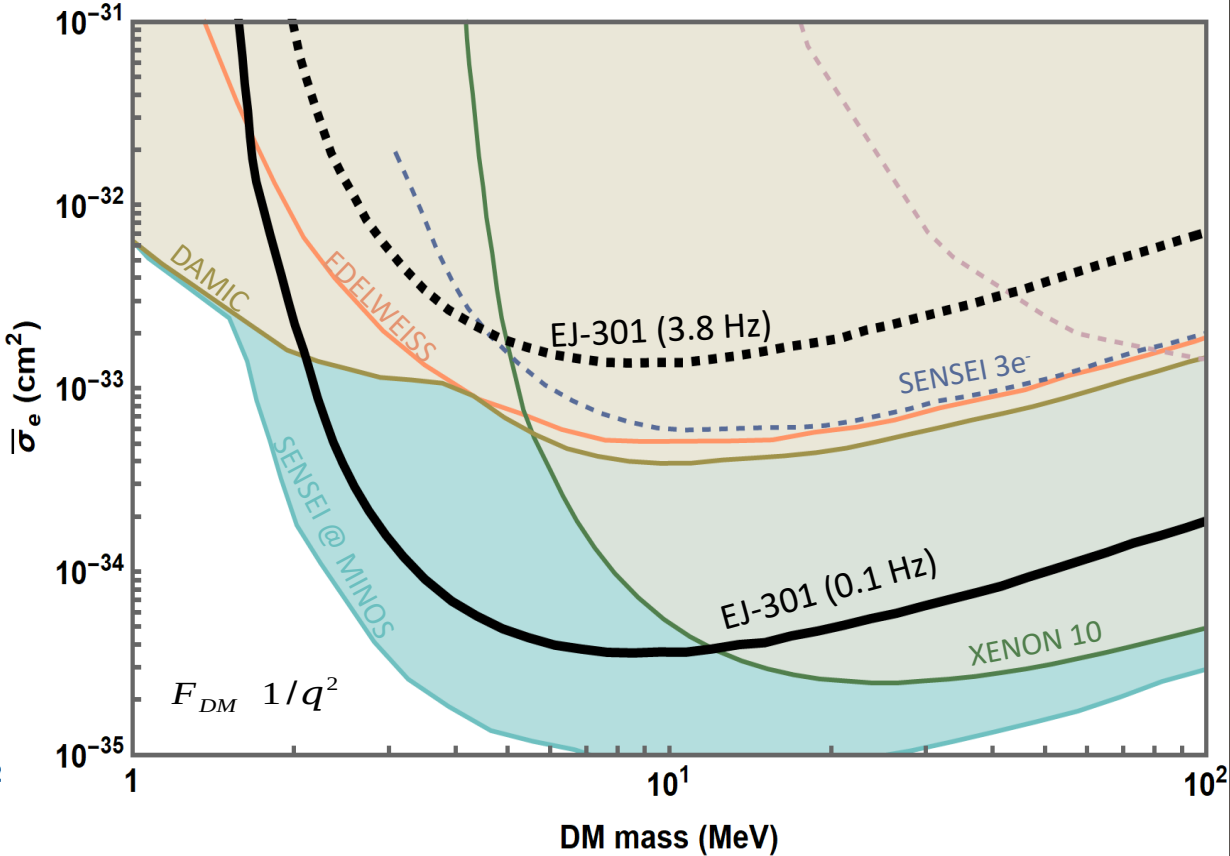# First Experimental Setup

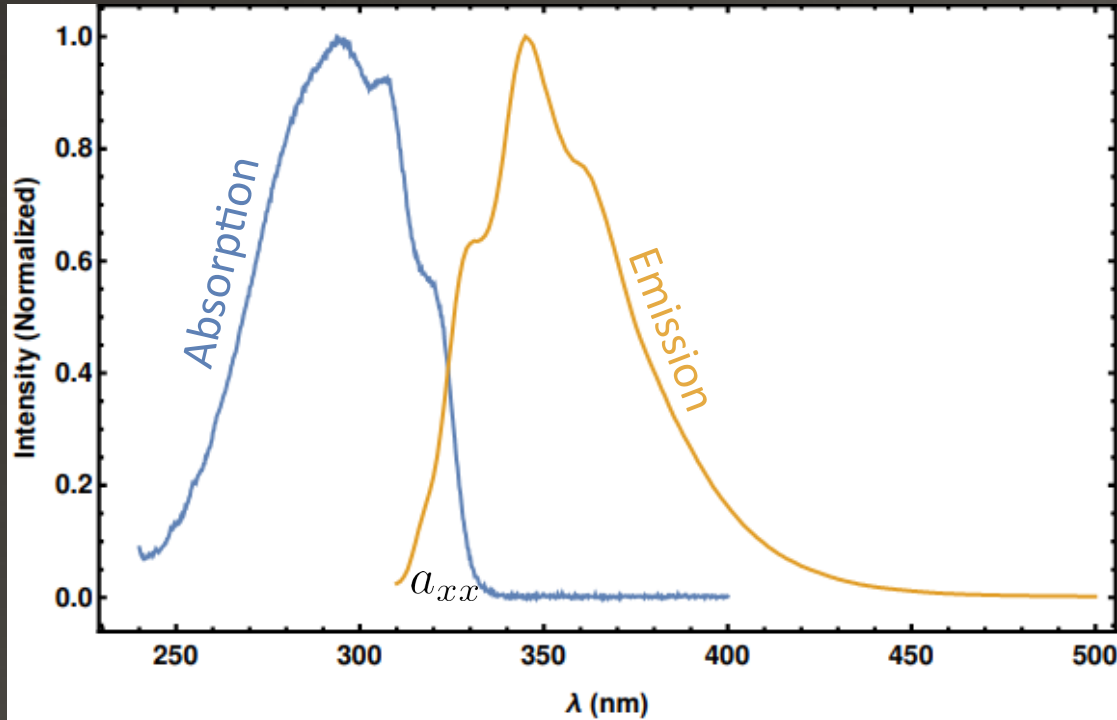Carlos Blanco August 30 2023

Results: EJ-301

(Contact interaction)
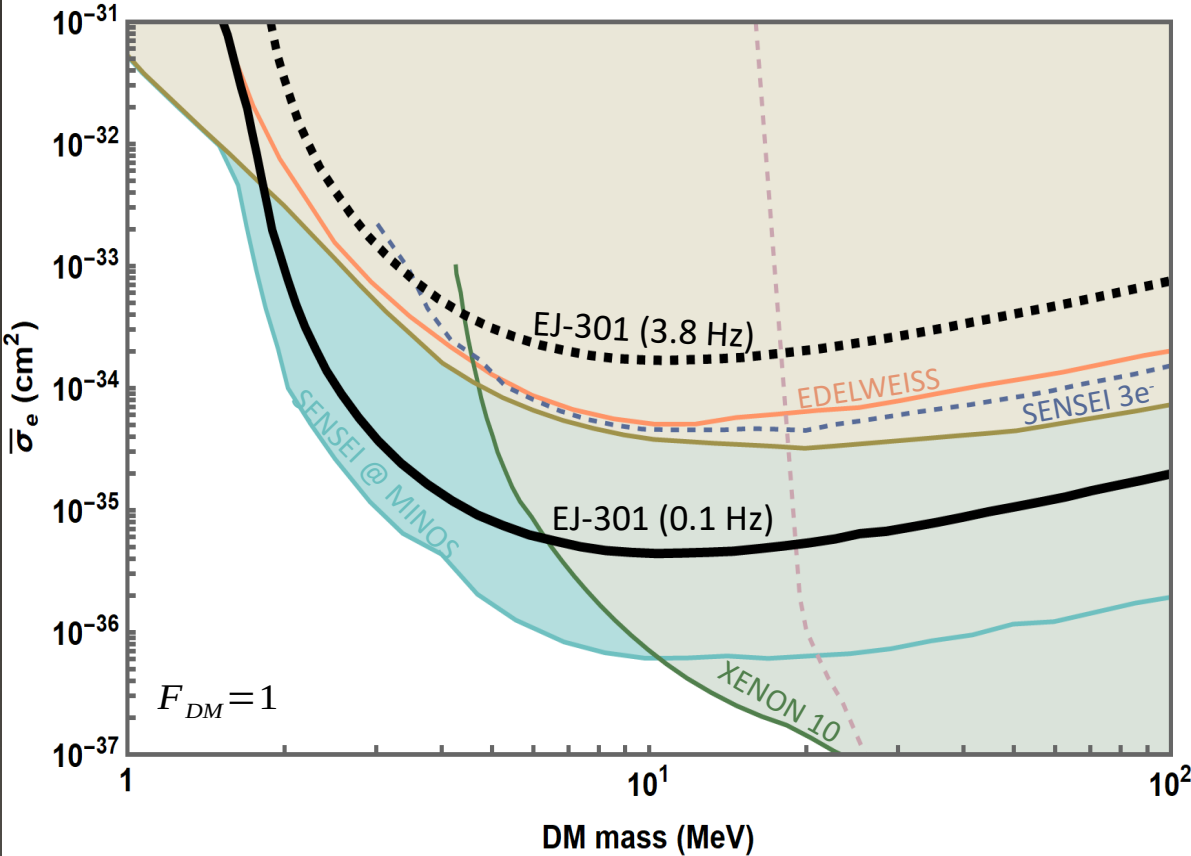
(Long-range interaction)

Blanco '19: 1912.02822

About 6 months from theory development to results!

Fluorescence with DM Works

Plot axes: Intensity (Normalized) vs λ (nm), with curves labeled **Absorption** and **Emission**, and point labeled a_{xx}.

<u>Now what we need is:</u>

Lower background

<u>Option 1</u>
Reduce background in the absorption step, i.e. selective excitation.

Molecular crystals have fundamentally anisotropic excitation probabilities. This leads to daily modulating signals from DM.
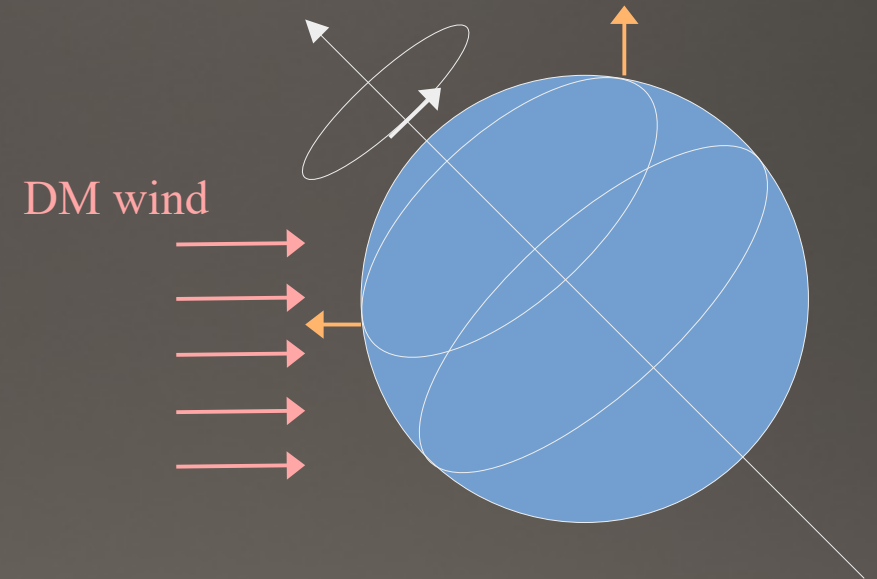
<u>Option 2</u>

Reduce background in the emission step, i.e. selective signal generation.

Quantum dots can produce a pair of time-coincident photons following excitation.
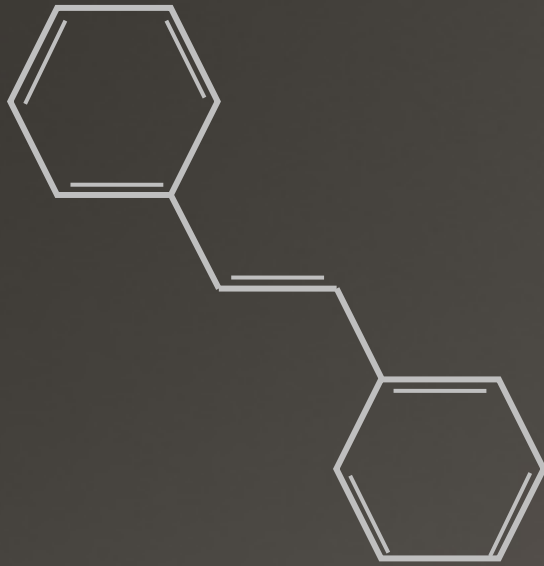
Directional Detection
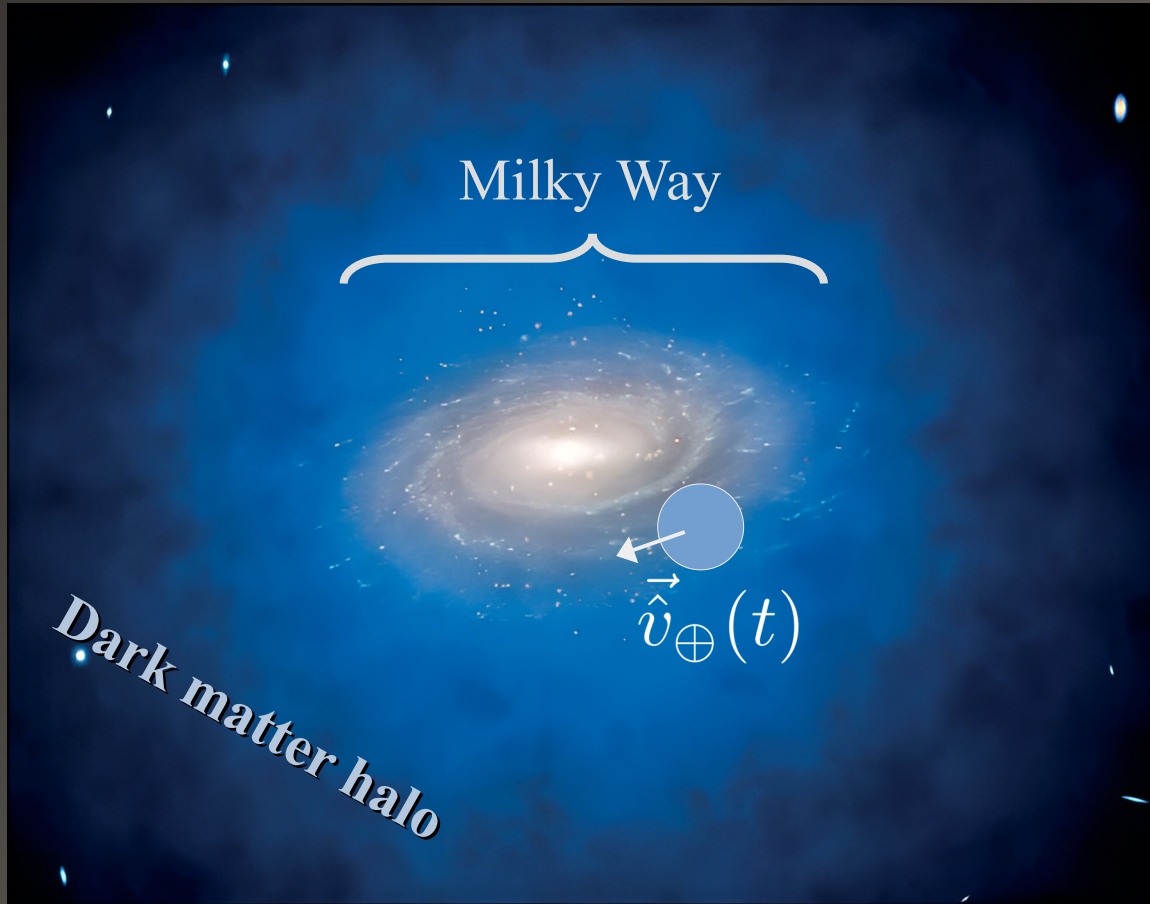
The earth experiences a dark matter "wind" in the direction of travel around the Milky Way
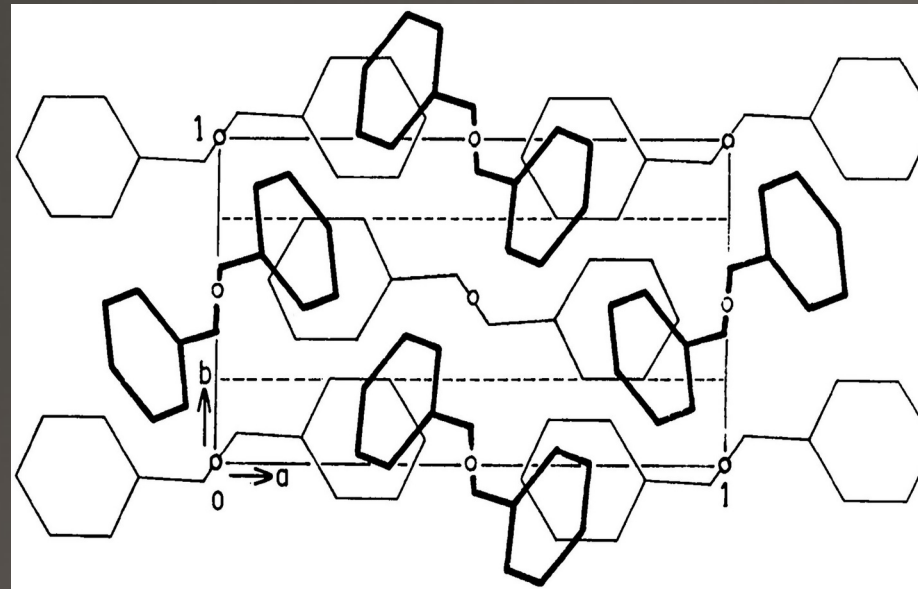
Change in relative orientation between detector and dark matter wind leads to **daily** modulation
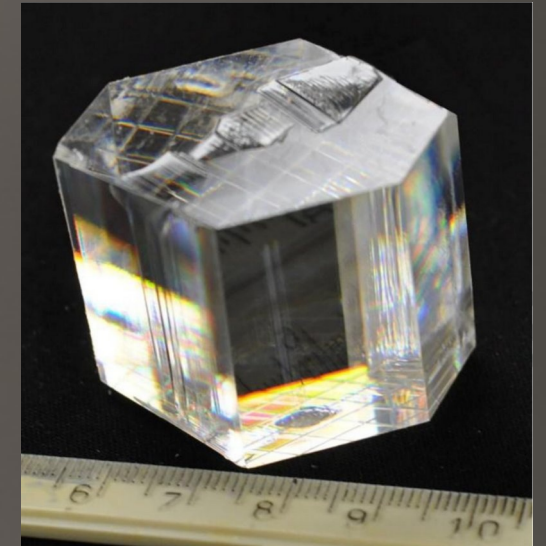
Trans-Stilbene

Carman, et.al. '18 (J. of Crystal Growth)

De-localized and planar network of double bonds

Molecular planes oriented in crystal lattice
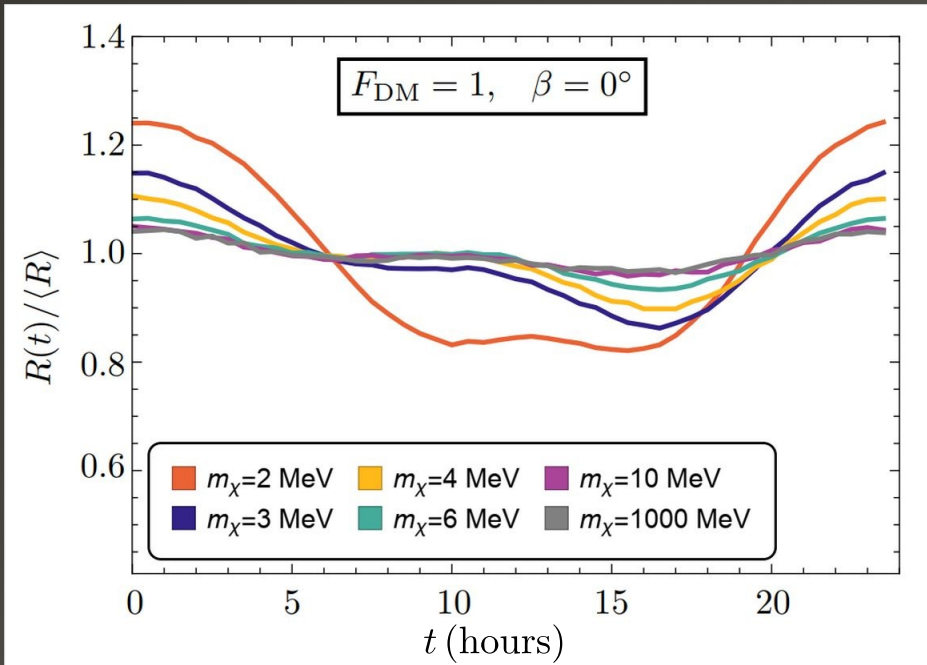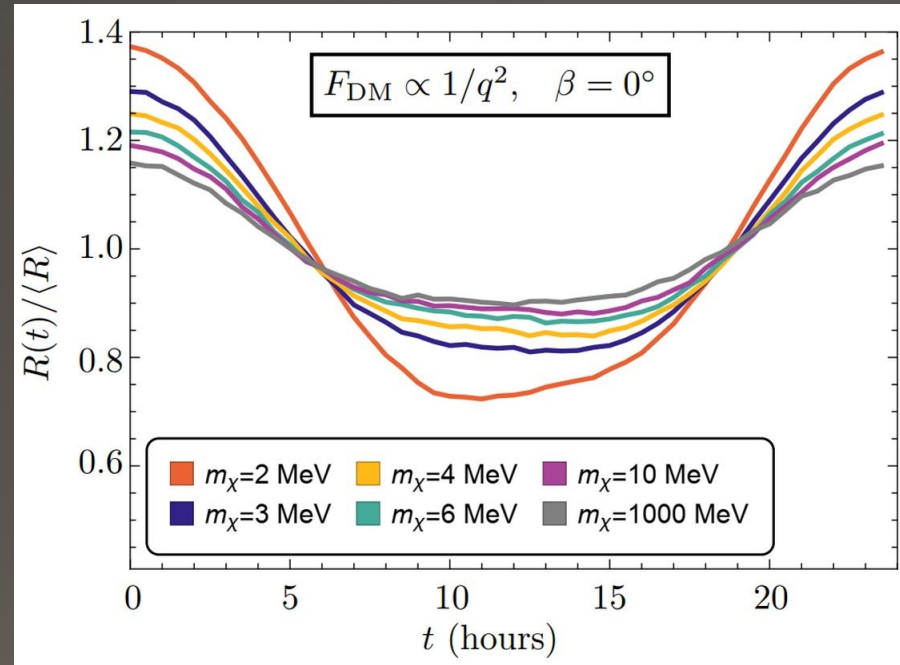
Large optical-quality crystals

Daily Modulation

(Contact interaction)

(Long-range interaction)

Predicted rate changes by up to 70% throughout the day.

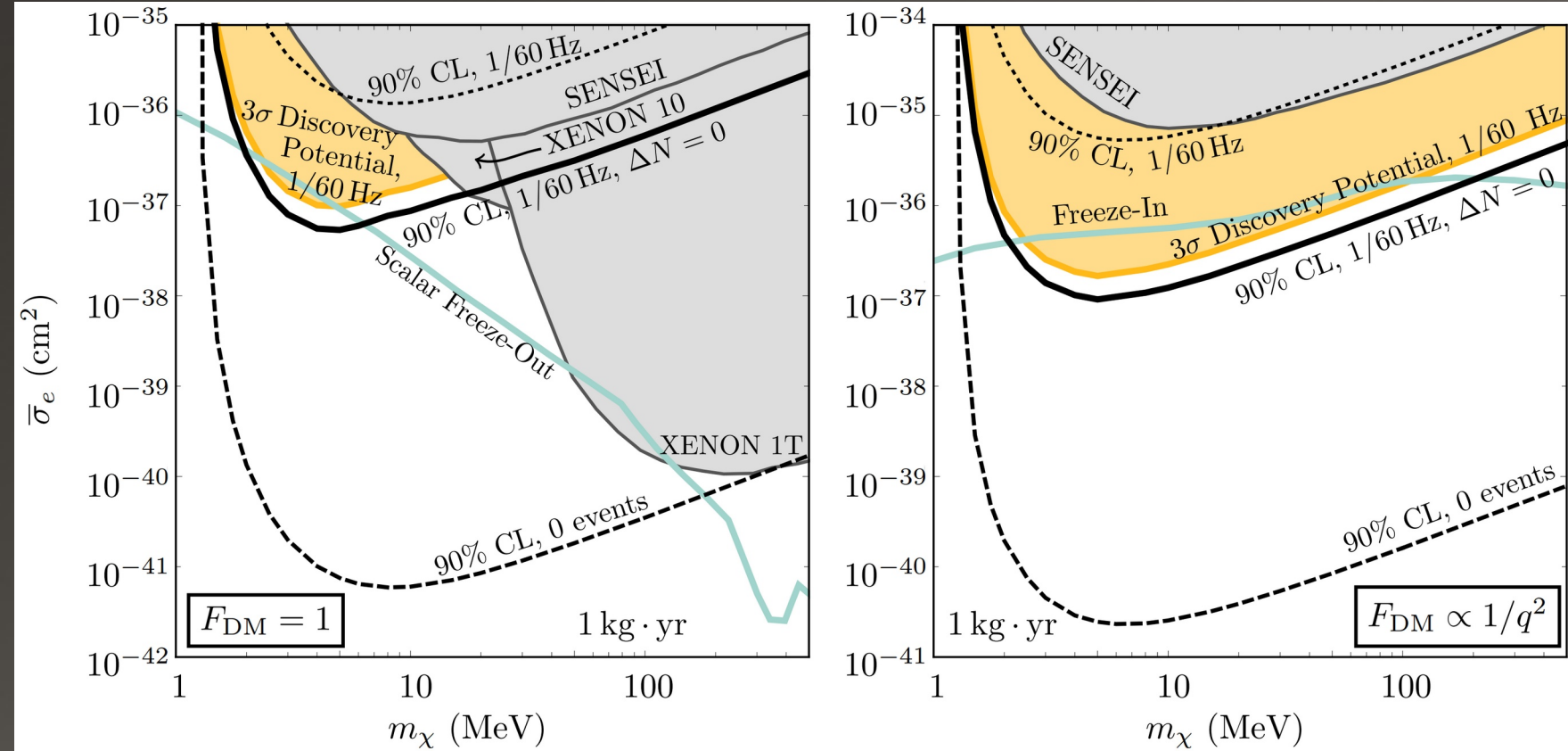That's a verifiable signal!

Blanco '21: 2103.08601

Modulation amplitude remains as high as 10% even at the highest masses. This is due to the fundamental anisotropy of the molecular form factor.

Sensitivity & Reach

(Contact interaction)

(Long-range interaction)

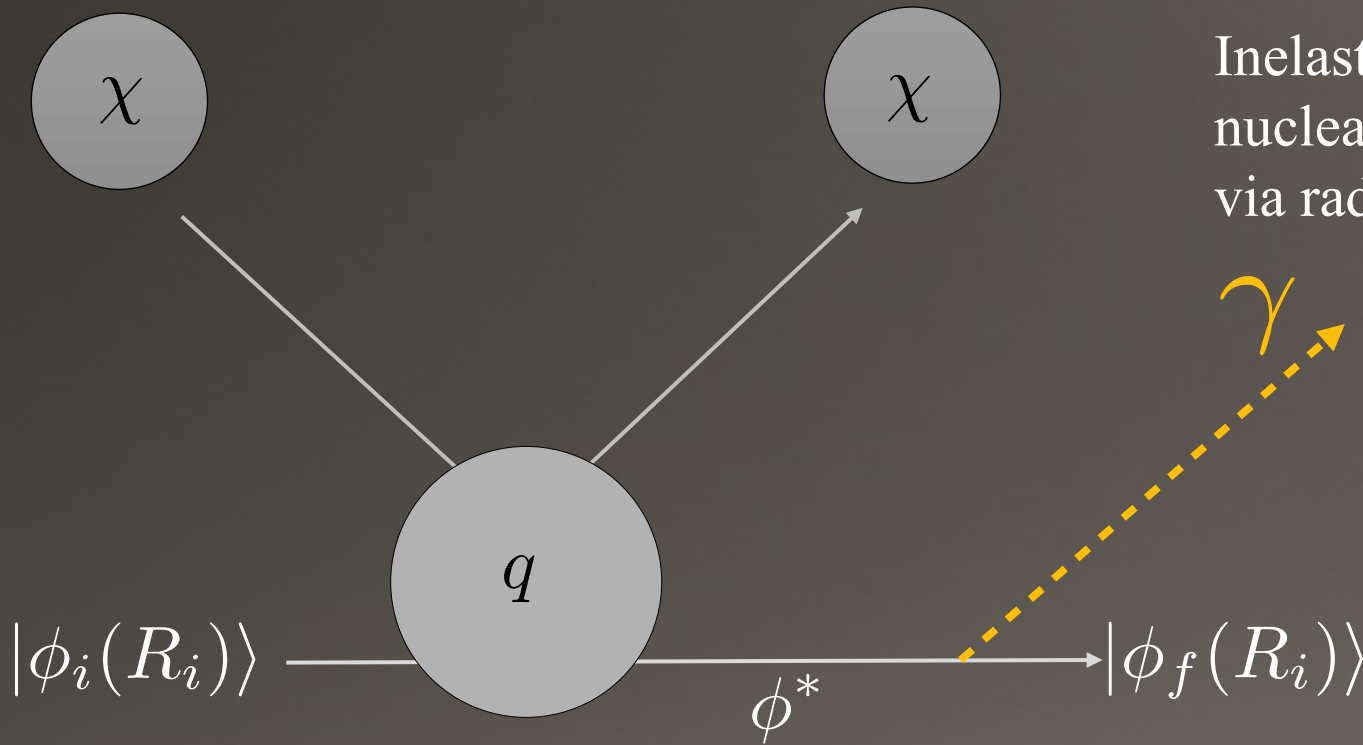Assuming realistic backgrounds

Exclusion w/o modulation

Discovery potential w/ mod.

Exclusion w/ modulation

Modulating signals improve sensitivity by about two orders of magnitude and provide the potential for discovery

*1kg of t-stilbene can probably be found within a few blocks of this room
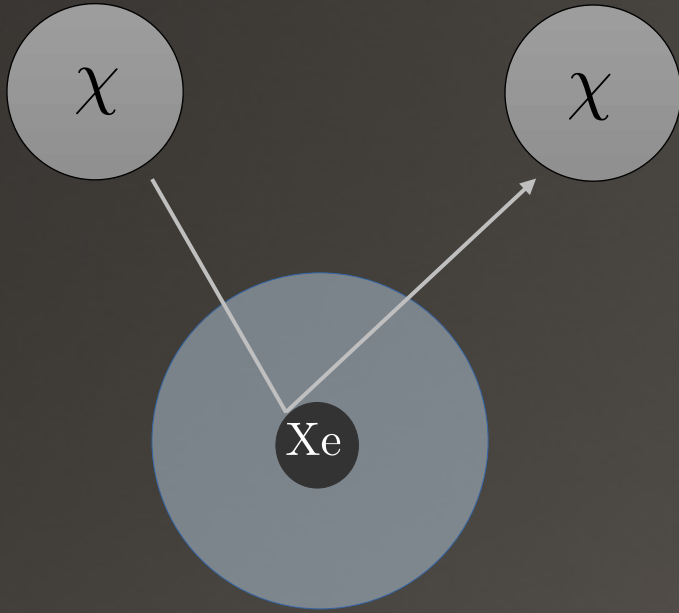
Blanco '21: 2103.08601

Nuclear Recoil: Photon Signal

Inelastic scattering or bosonic absorption on nuclear states leads to an excitation that decays via radiative emission.

χ

χ

γ

q

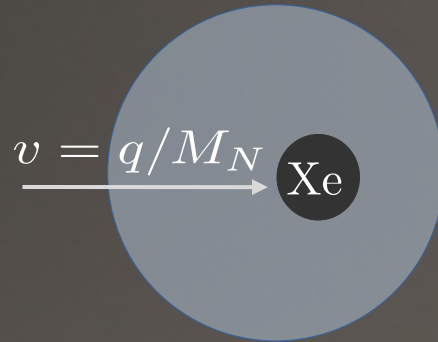$|\phi_i(R_i)\rangle$ ———— ϕ^* ————→ $|\phi_f(R_i)\rangle$

Nuclear scattering

$$\Delta E \sim \mathcal{O}(\text{few eV}) \left(\frac{m_\chi}{100\,\text{MeV}}\right)^2 \left(\frac{m_N}{130\,\text{GeV}}\right)^{-1}$$
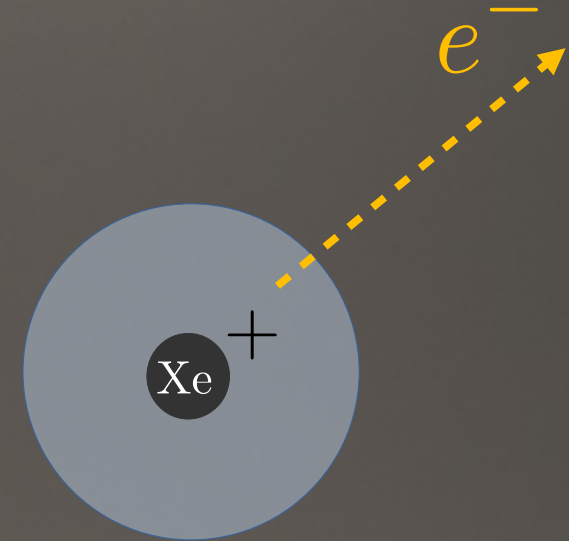
The Migdal Effect: Atoms

$$|\psi_i\rangle \sim e^{i\frac{m_e}{M_N}\vec{q}\cdot\vec{r}}\psi_{\mathrm{AO}}(r_\beta)$$

χ χ

e^-

Xe

$v = q/M_N$ Xe

Xe $+$

Initial nuclear recoil

Nucleus recoils faster than motion of electrons

Electronic transition to ionized state

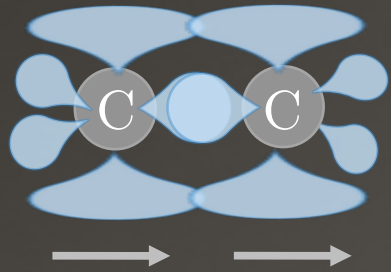$$f_{i\to f} \approx \frac{m_e}{M_N}\vec{q}\cdot\langle\vec{r}\rangle_{i\to f}$$

The Migdal effect in atoms has been invoked in e.g. Xenon to extend the sensitivity of noble liquid detectors to lower masses.

Migdal transition probability is suppressed by kinematic mis-match.

The Molecular Migdal Effect(s)
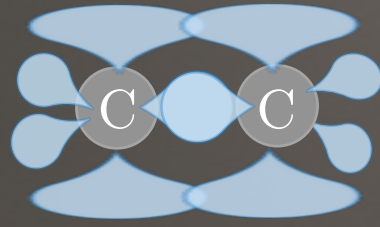

Center of mass recoil (CMR) effect

Caused by center of mass motion

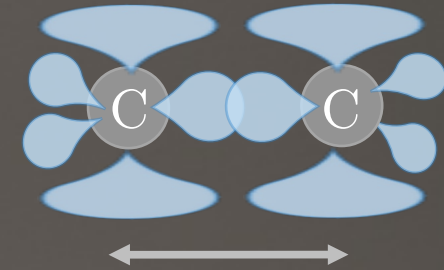COM recoil effect is the molecular analog of the semiclassical Migdal effect

$$P_{CMR} \sim \frac{m_e}{M_{mol}}$$

Suppressed by kinematic factor due to moving the whole molecule.

Non-adiabatic coupling (NAC) effect
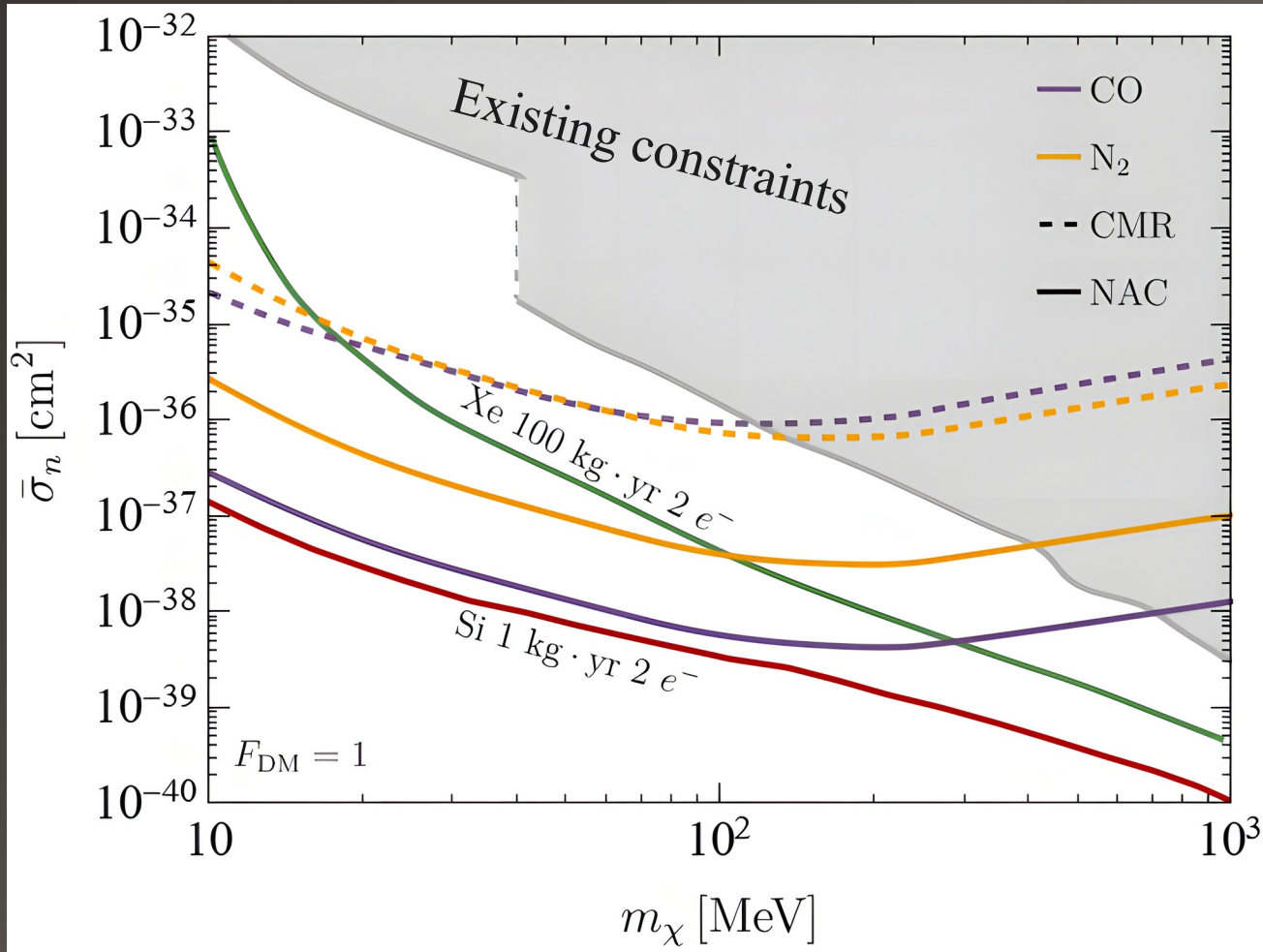
Caused by relative motion

NAC caused by effects beyond Born-Oppenheimer approximation

$$P_{NAC} \sim \frac{m_e}{M_N}$$

Suppressed by kinematic factor due to moving a single atom.

Blanco '22: 2208.09002
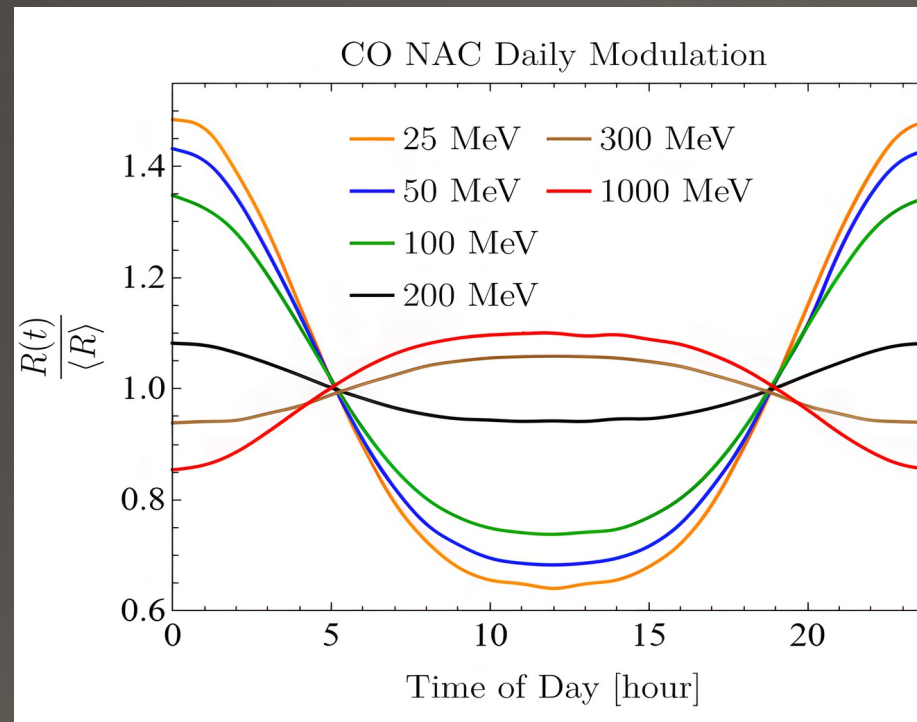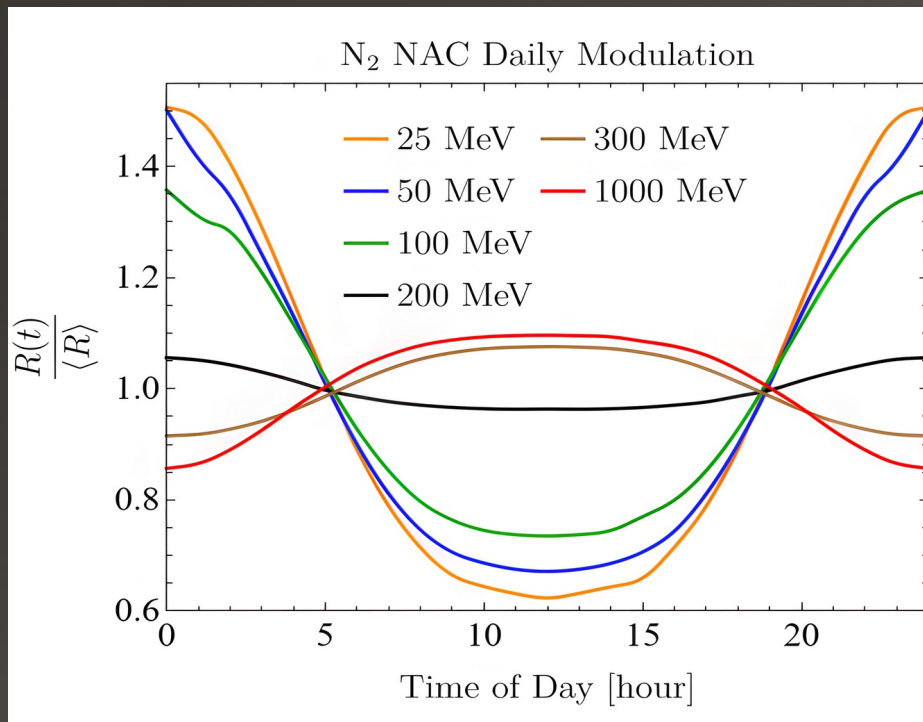
The Molecular Migdal Effect(s)

(Contact interaction)

Si rate is calculated using the *CMR*-equivalent Migdal effect.
Is there an *NAC*-equivalent in Si?

Center of mass recoil effect is predicted to be subdominant at all masses.

Non-adiabatic coupling effect is predicted to dominate due to favorable kinematic factor.

Simplest molecular models already competitive.
Is there an optimal molecular target?

Blanco '22: 2208.09002

Directional Molecular Migdal Effect

N$_2$ NAC Daily Modulation

- 25 MeV
- 50 MeV
- 100 MeV
- 200 MeV
- 300 MeV
- 1000 MeV

CO NAC Daily Modulation

- 25 MeV
- 50 MeV
- 100 MeV
- 200 MeV
- 300 MeV
- 1000 MeV

$\frac{R(t)}{\langle R \rangle}$

Time of Day [hour]

Predicted rate changes by up to 80% throughout the day.

The daily modulation phase is mass dependent.

Blanco '22: 2208.09002

Persistent daily modulation at large dark matter mass is generically predicted for the molecular Migdal effects.

We predict that the same class of molecules that make good directional detectors for electron scattering will also be ideal for nuclear scattering because of the directional molecular Migdal effects.

Fluorescence with DM Works
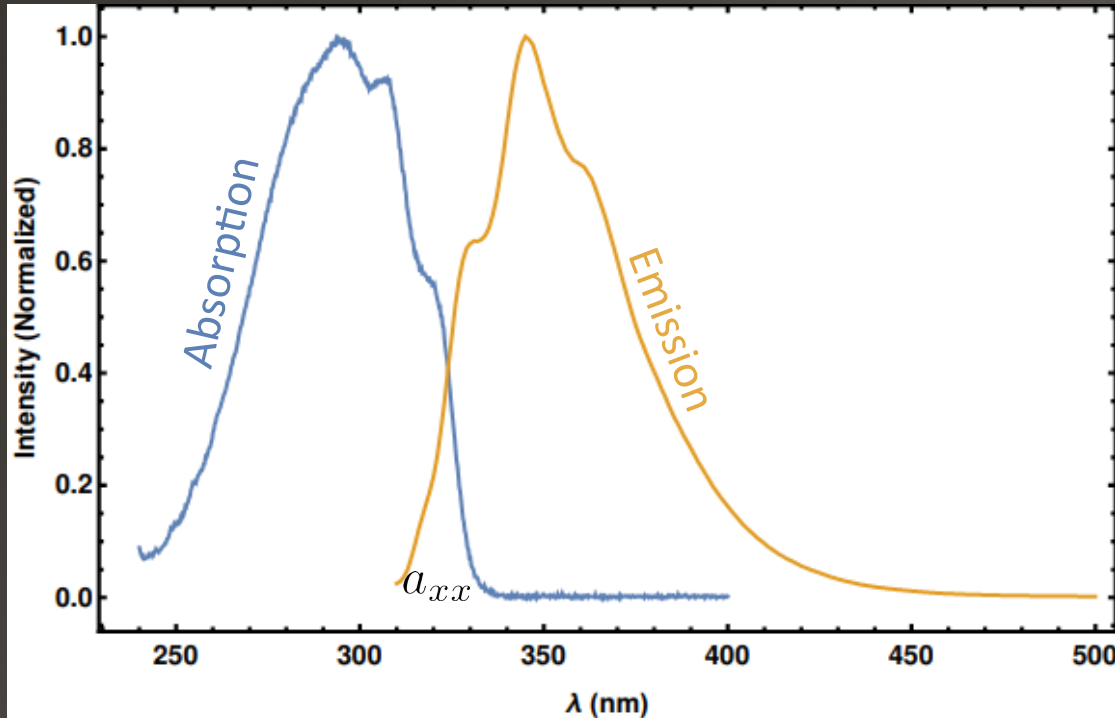
Now what we need is:

Lower background

Option 1
Reduce background in the absorption step, i.e. selective excitation.

Molecular crystals have fundamentally anisotropic excitation probabilities. This leads to daily modulating signals from DM.
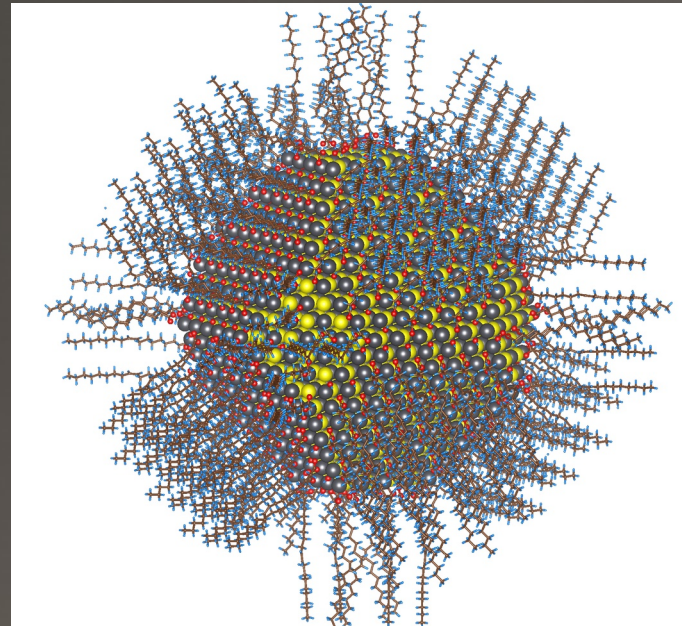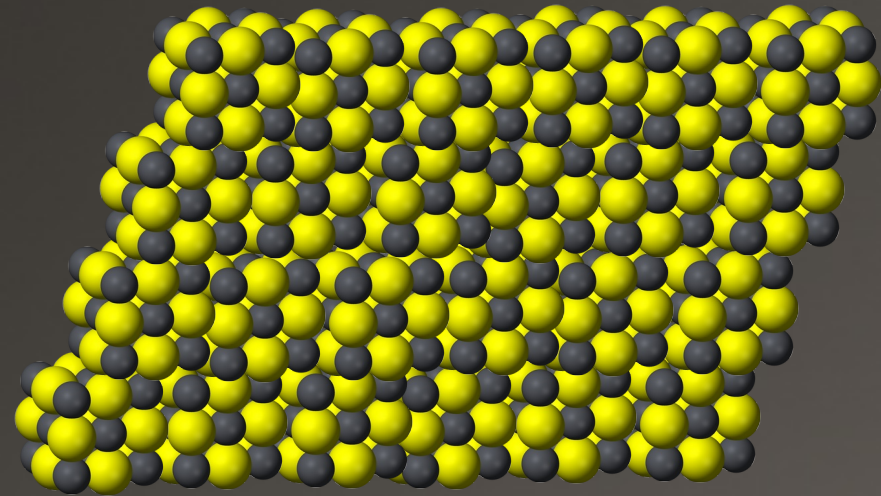
Option 2
Reduce background in the emission step, i.e. selective signal generation.

Quantum dots can produce a pair of time-coincident photons following excitation.

What are Quantum Dots?

Quantum confinement affects the long-wavelength physics

Quantum confinement

Zherebetskyy et al., Science 344, 1380 (2014)

$$R \to \infty \ \mathrm{nm}$$

$$R \sim \mathcal{O}(\mathrm{few \ nm})$$

$$|\psi_i\rangle \sim u_{\mathrm{Bloch}}(r)e^{ik\cdot r}$$

$$|\psi_i\rangle \sim u_{\mathrm{Bloch}}(r)\psi_{\mathrm{bound}}(r)$$

Conduction

Conduction

$$\Delta E_g$$

$$\Delta E_{QD} > \Delta E_g$$

Valence

Valence

$$E(k)$$

Quantum Dots
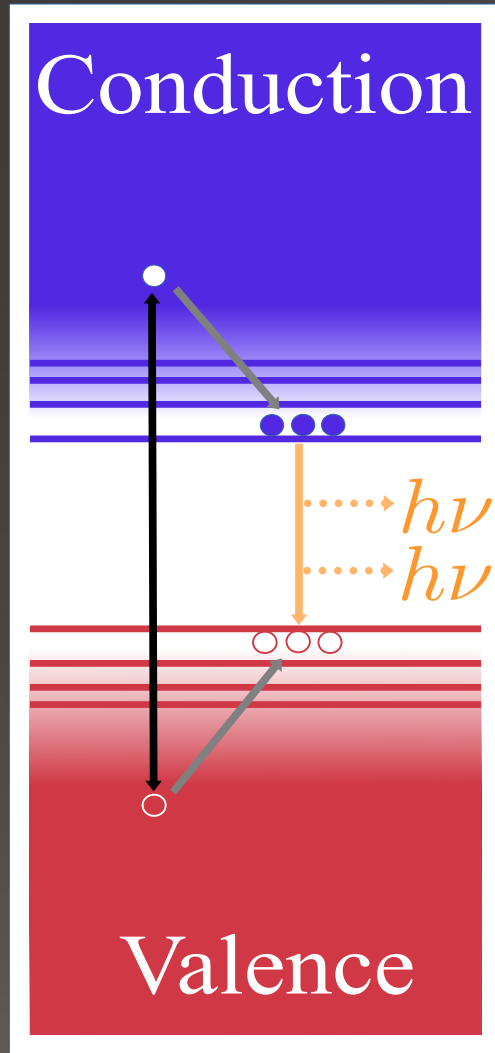

Absorption: Creation of a "hot" exciton – an electron/hole pair with energy significantly larger than the bandgap

Non-Radiative Transition: Multi-exciton generation when energy is greater than twice the bandgap creates several band-edge excitons.

Emission: Radiative recombination of several band-edge excitons producing several coincident photons
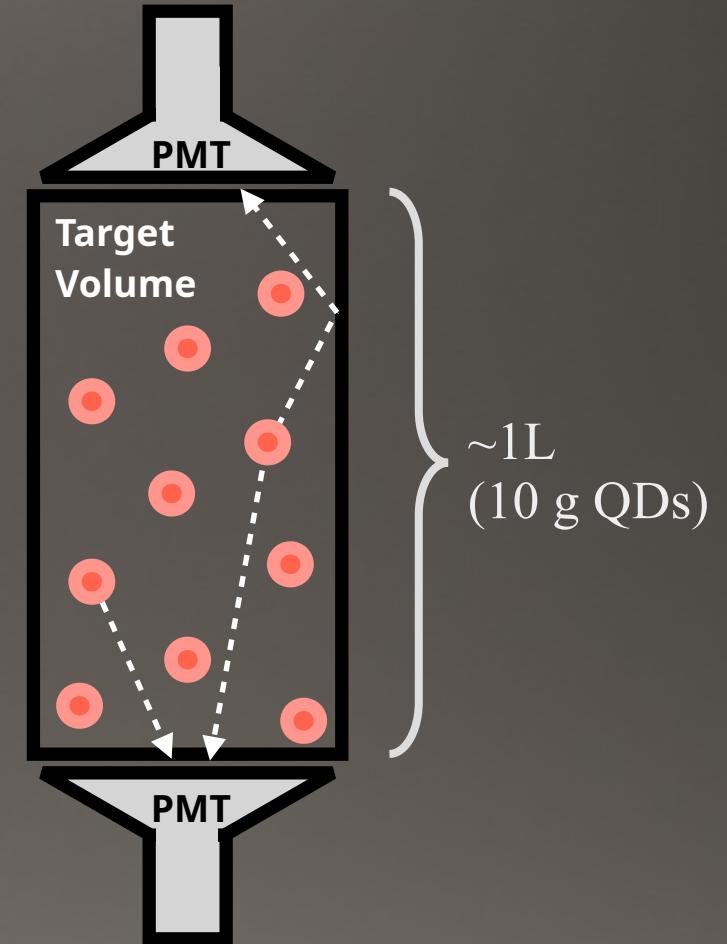
PbS Quantum Dots

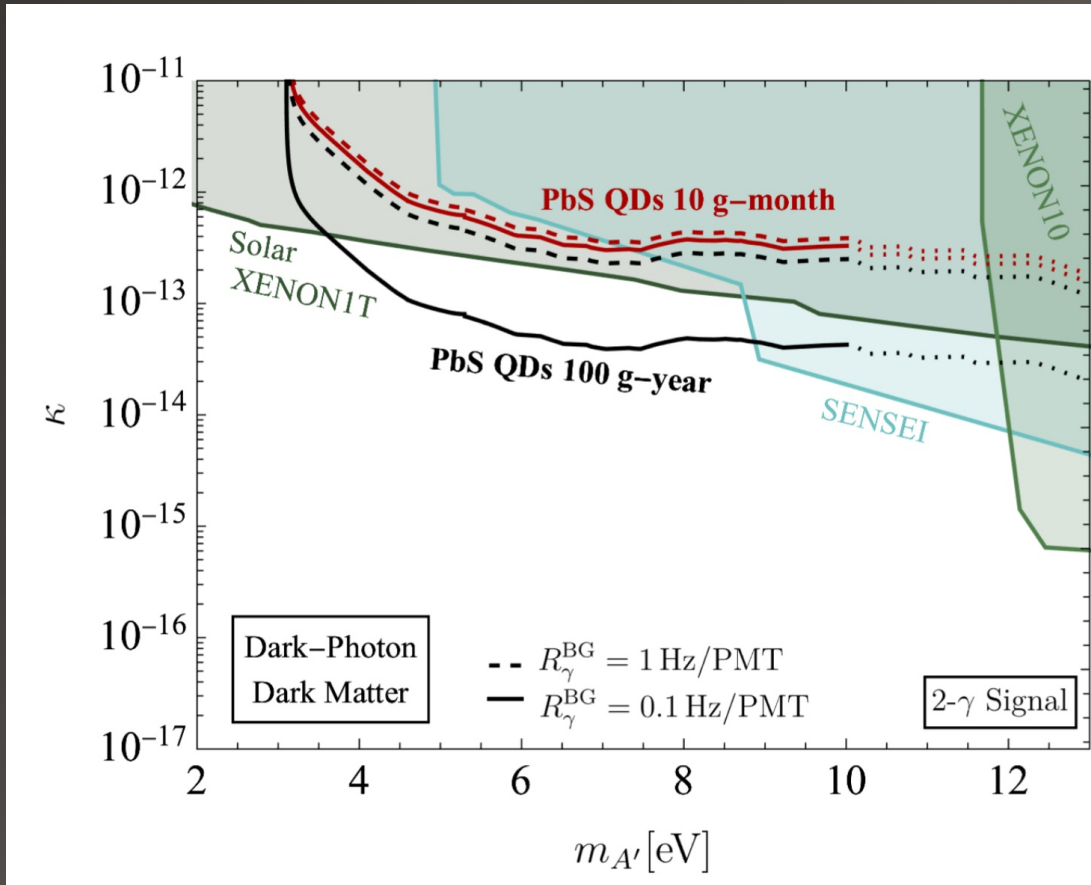(Contact interaction)

(Long-range interaction)
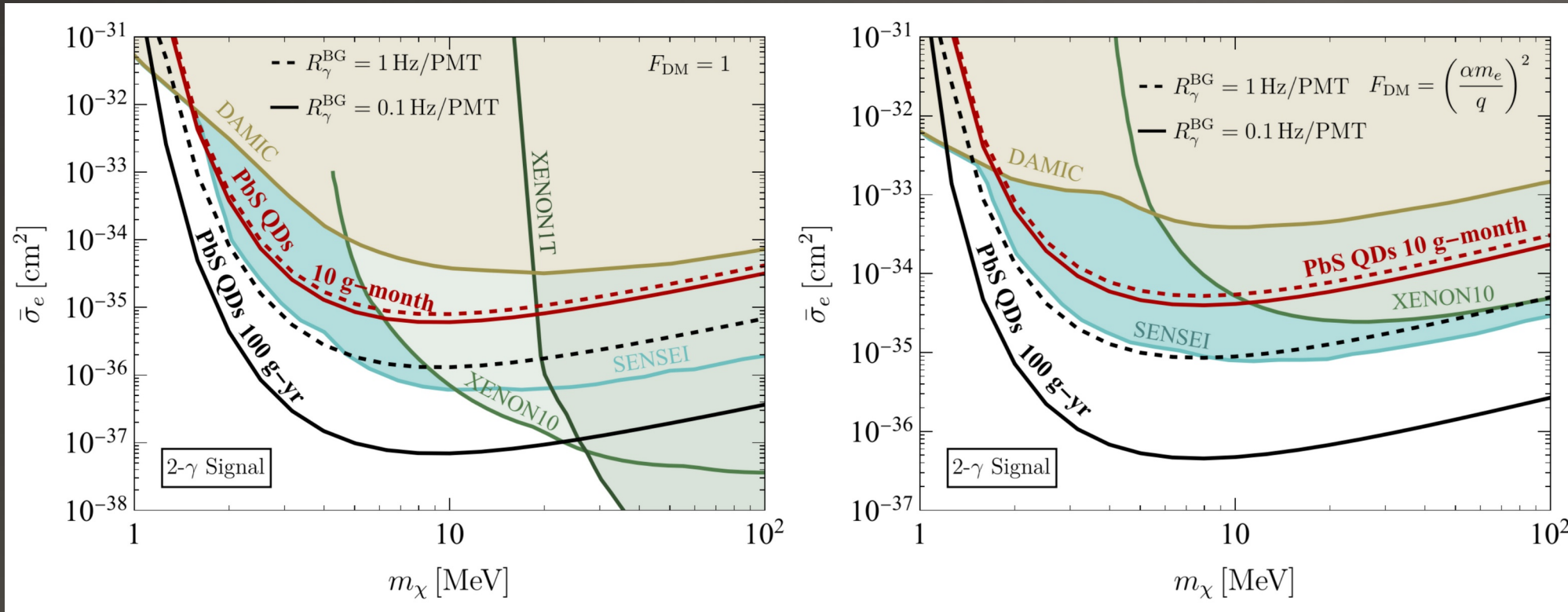
Essentially
background free
@ this scale

Blanco '22: 2208.05967

Assuming a realistic dark rate for the photodetectors, QD-based detectors using existing technology would be deployed and easily scaled to overtake existing limits.

PbS QDs

Dark photon kinetic coupling

Blanco '22: 2208.05967

In the case of eV-scale dark photon absorption, we can use existing *data* to predict the sensitivity of QD-based detectors.

Key conclusions of QD analysis

1) The interaction rate in a semiconductor generated by DM is the same if the semiconductor is *monolithic* or *nanoscopically* disperse.

2) In a QD-based experiment, the readout is independent of the target.

3) The signal can be tuned through control of quantum confinement.

Deployment

LETTER OF INTENT:

QUAntum dot **D**ark matter **R**ecoil detection with **A**balone photosensors (QUADRA)

Carlos Blanco[1,2], Jan Conrad[2], Rouven Essig[3], Alfredo Davide Ferella[5], Tim Linden[2], Jörn Mahlstedt[2], and Val Zwiller[4]

[1]*Department of Physics, Princeton University, Princeton, NJ 08544, USA*
[2]*Stockholm University and The Oskar Klein Centre for Cosmoparticle Physics, Alba Nova, 10691 Stockholm, Sweden*
[3]*C. N. Yang Institute for Theoretical Physics, Stony Brook University, USA*
[4]*Department of Applied Physics, Royal Institute of Technology, Roslagstullsbacken 21, 114 21 Stockholm, Sweden*
[5]*Department of Physics and Chemistry, University of L'Aquila, 67100 L'Aquila, Italy and INFN-Laboratori Nazionali del Gran Sasso and Gran Sasso Science Institute, 67100 L'Aquila, Italy*
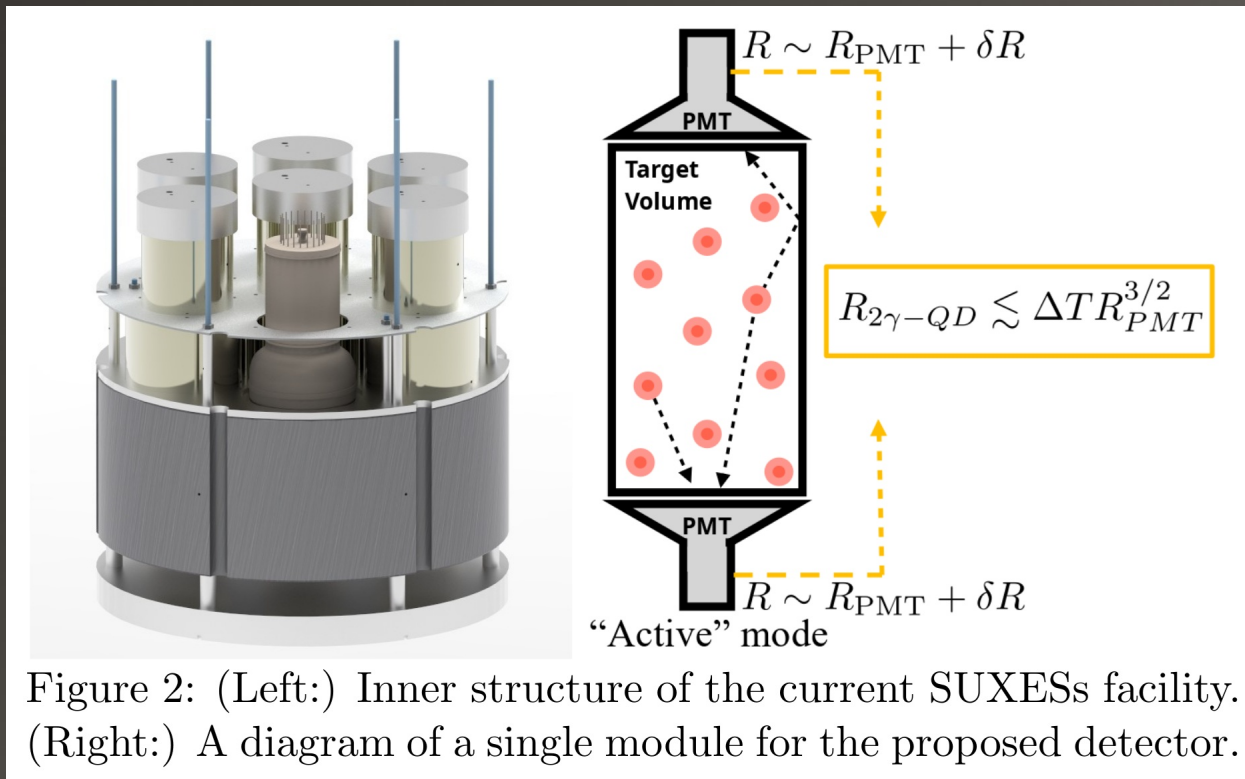
October 31, 2022

Deployment

Figure 2: (Left:) Inner structure of the current SUXESs facility. (Right:) A diagram of a single module for the proposed detector.
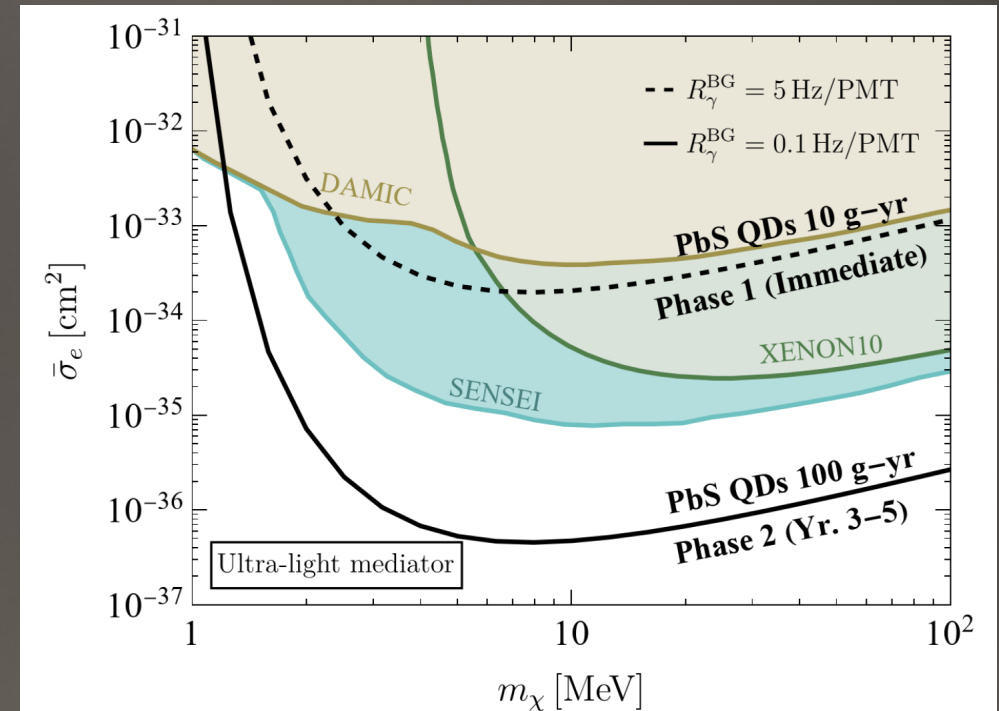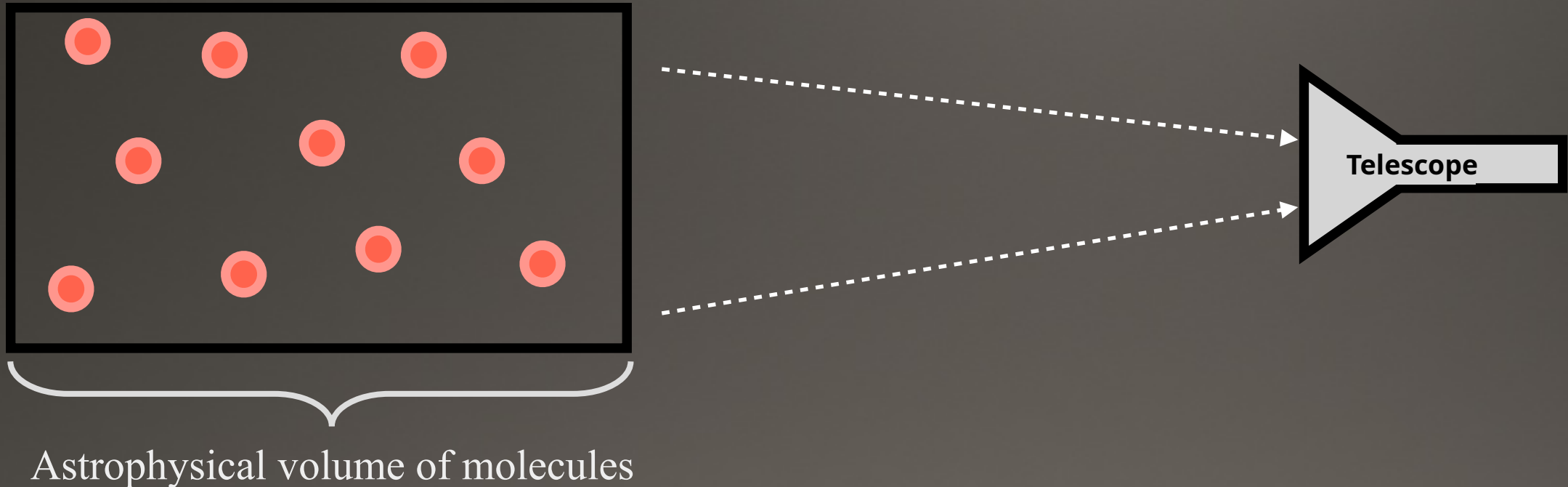

Figure 1: The sensitivity of a QD detector looking for coincident signals, for DM models with a light mediator coupling to electrons. Shaded are existing limits. Fig. adapted from Ref. [1]
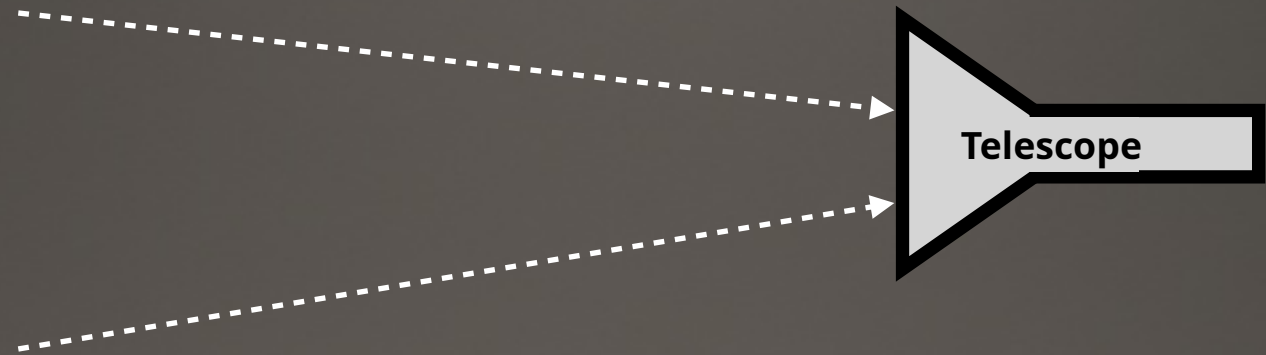
Beyond direct detection

Telescope

Astrophysical volume of molecules

We can use the same theoretical techniques that we've developed to predict rates in *astrophysical* objects

Blanco '22 (ArXiv: 2211.05787)
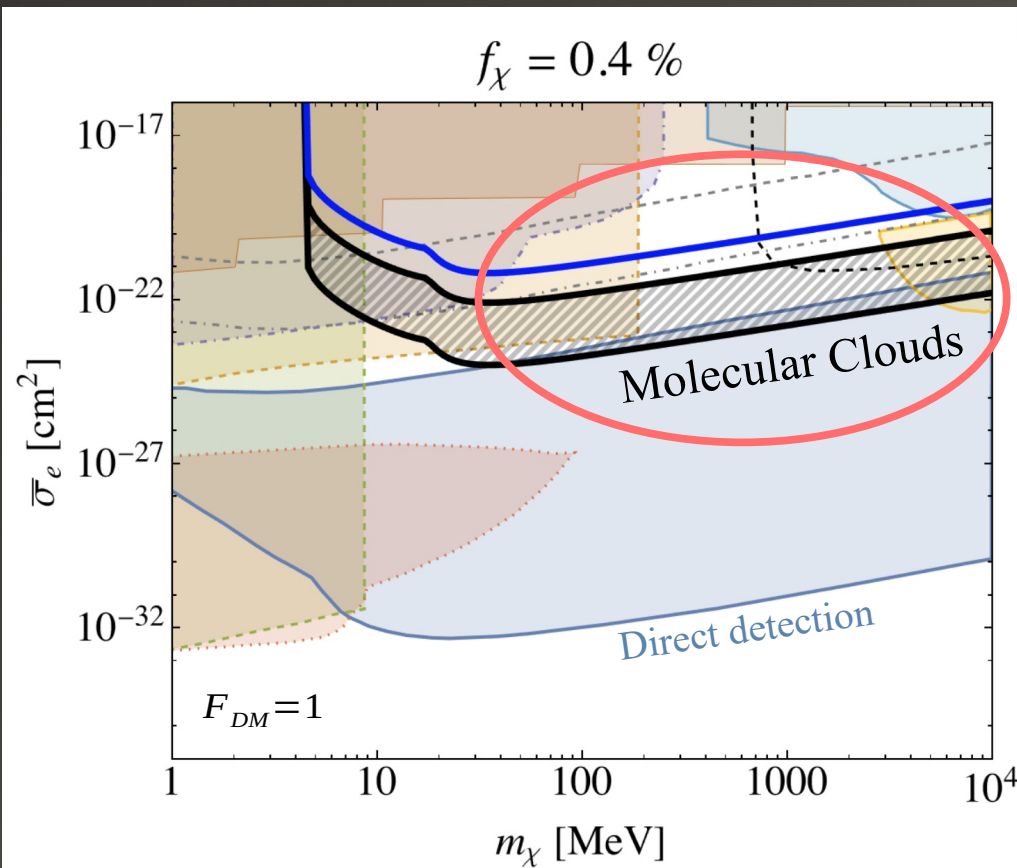
Beyond direct detection
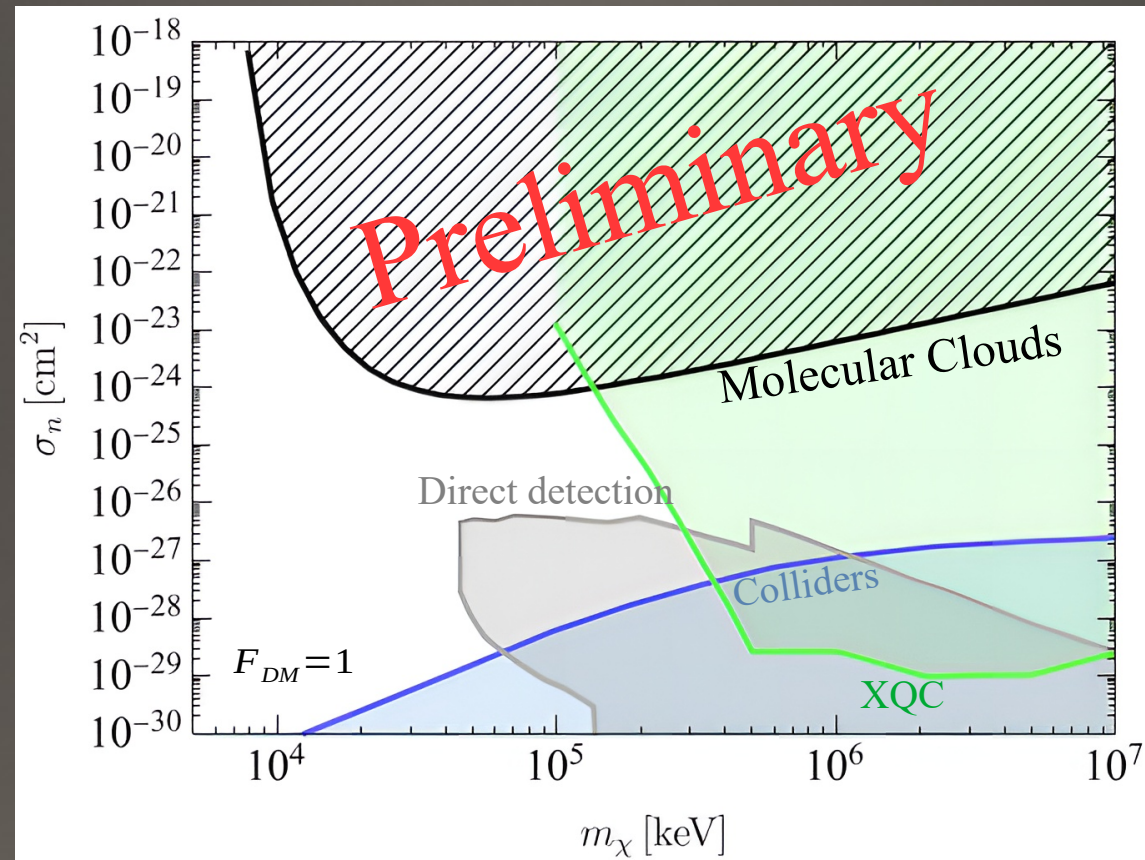

Cold molecular cloud

Telescope

We can use the same theoretical techniques that I've developed to predict rates in detectors to predict rates in *astrophysical* objects

Dark matter in Molecular Clouds

Blanco '22 (ArXiv: 2211.05787)

The Molecular Migdal effect(s) is *space*

Molecular cloud ionization (Thick lines) can constrain almost all remaining parameter space for a *strongly-coupled* subcomponent of DM which would never make it to other detectors.

Conclusions

1) Dark matter remains one of the central mysteries in modern cosmology and particle physics.

2) We have done an extremely effective job looking for WIMPs, now we must look beyond.

3) By developing the formalism that describes the interaction between dark matter and molecules or nano-materials, we can propose detection strategies capable of *delving deep* and *searching wide* across the dark matter parameter space.

4) This remains one of the few ways to probe high-energy physics at the bench-top scale.

5) Future hybrid methods may bring together both strategies giving multiplicative improvements to sensitivity.

Acknowledgements

- Collaborators & colleagues: Yoni Kahn, Ben Lillard, Juan Collar, Jesus Perez-Rios, Rouven Essig, Hari Ramani, Oren Slone, Dan Baxter, Marivi Fernandez-Serra, Sam McDermott, Ian Harris (In no particular order)

Dark matter in Molecular Clouds

~ 0.5 ly

Very dense and cold molecular clouds are almost entirely opaque.

$$n_{H_2} \sim O(10^2)\mathrm{cm}^{-3}$$

Ionization from CR produces ionization fraction: ζ^{H_2}

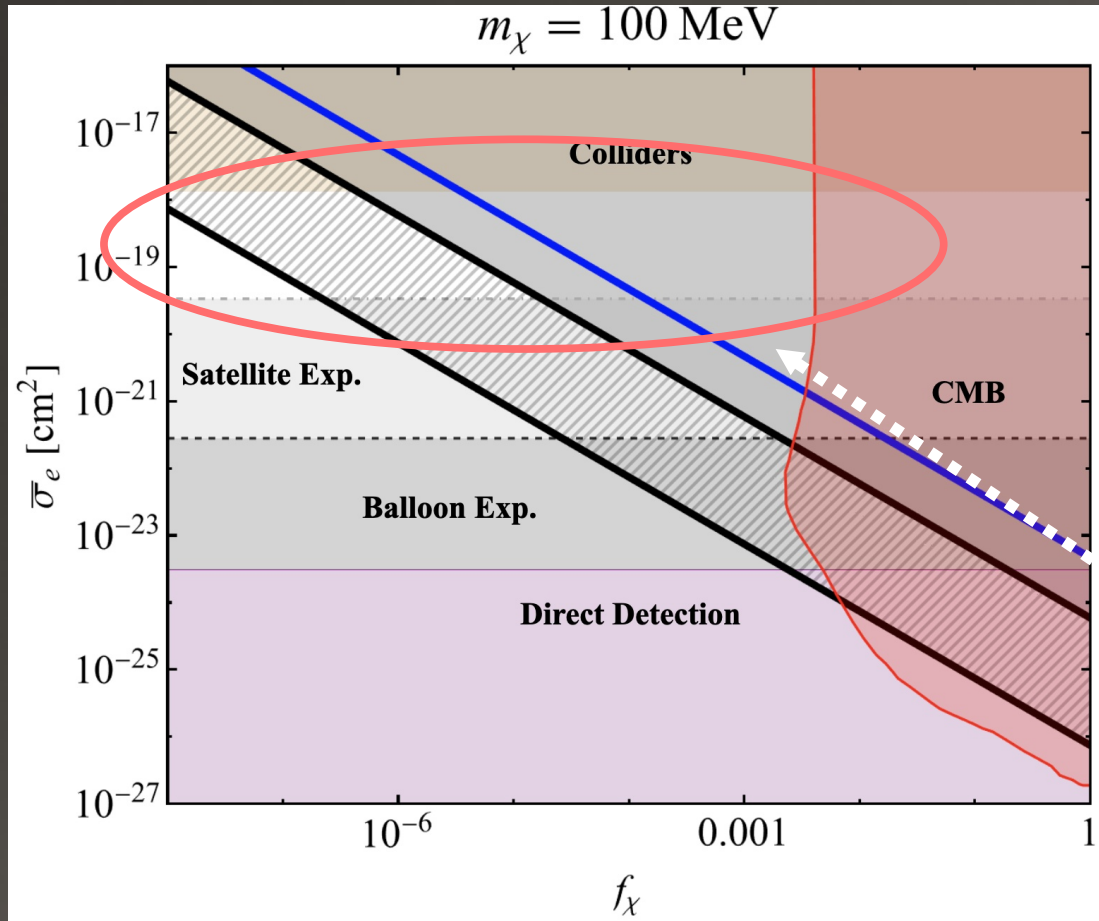$$\mathrm{CR} + \mathrm{H}_2 \to \mathrm{CR} + \mathrm{H}_2^+ + \mathrm{e}^-$$

This is well measured through astro-spectroscopy of tracer molecules (line intensity measurements)

However, DM annihilation into ionizing SM particles can also produce ionized fraction

$$\zeta_i^{H_2} = 2\pi \int \frac{dN_i}{dE}(E)\sigma_i(E)dE$$

Dark matter in Molecular Clouds

$m_\chi = 100\,\mathrm{MeV}$

Constraints on DM w/ ultra-light mediator from dense (black) and diffuse (blue) molecular clouds. The hatched region represents the uncertainty in our bounds coming from the uncertainty in the inferred CR ionization rate coming from gas depletion onto grain surfaces.

There would otherwise be an open window of parameter space where the dark matter is too strongly-coupled to be visible even by satellite experiments.

Blanco '22 (ArXiv: 2211.05787)

Daily Modulation: Small Mass
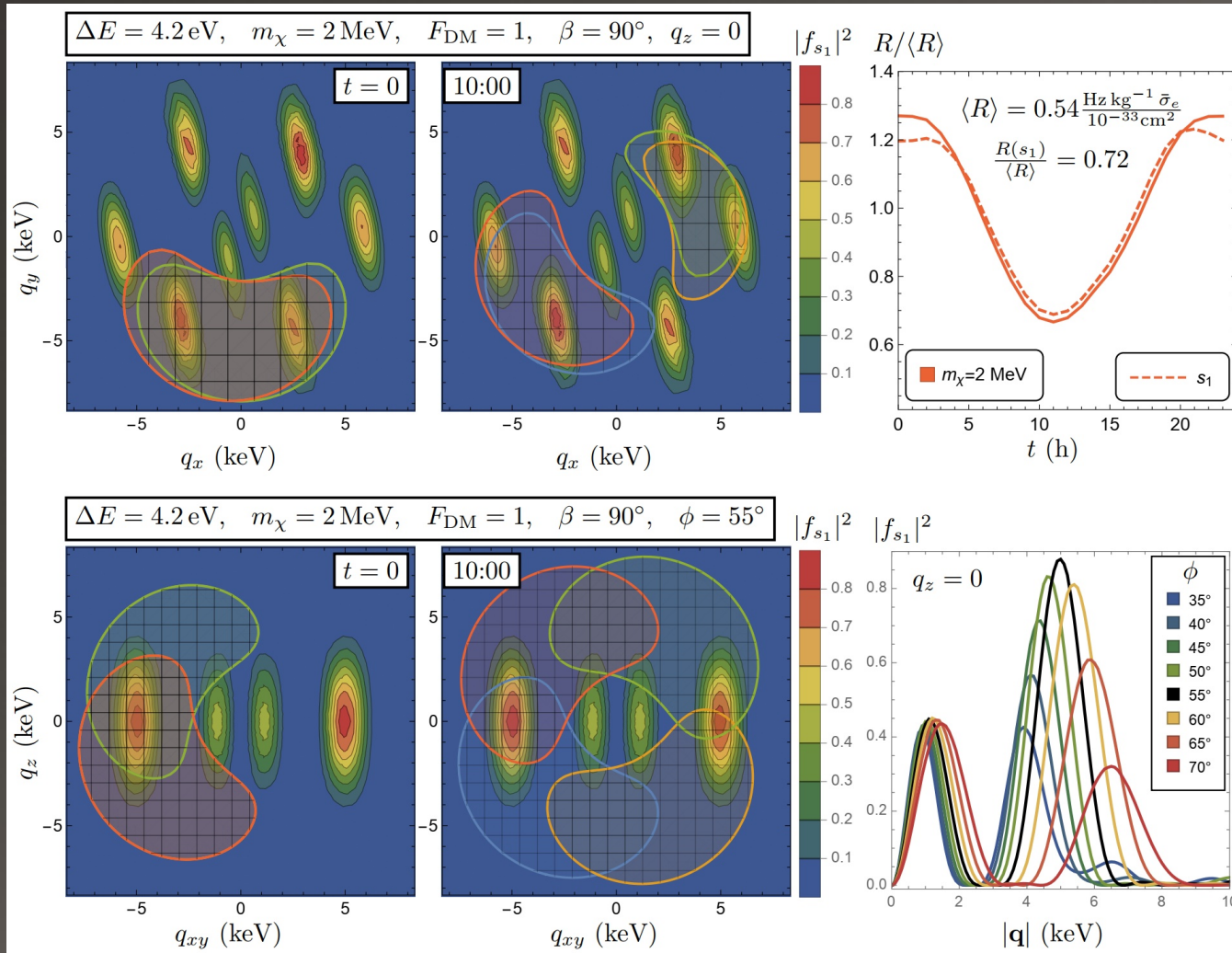
Molecular form factors and modulating rates for DM masses near threshold, $m_\chi = 2$ MeV. In the contour plots, the gridded shaded regions indicate the kinematically accessible momentum transfers $\vec{q}$ for the four molecules that comprise the unit cell of the crystal, shown at $t = 0$ and $t = 10$ h. Here, $\vec{q}$ is given in the molecular basis, $q_x = \vec{q} \cdot \hat{\vec{L}}$, $q_y = \vec{q} \cdot \hat{\vec{M}}$, and the kinematically accessible region is defined by $v_-(\vec{q}) < v_{\text{esc}}$.

Daily Modulation: Large Mass
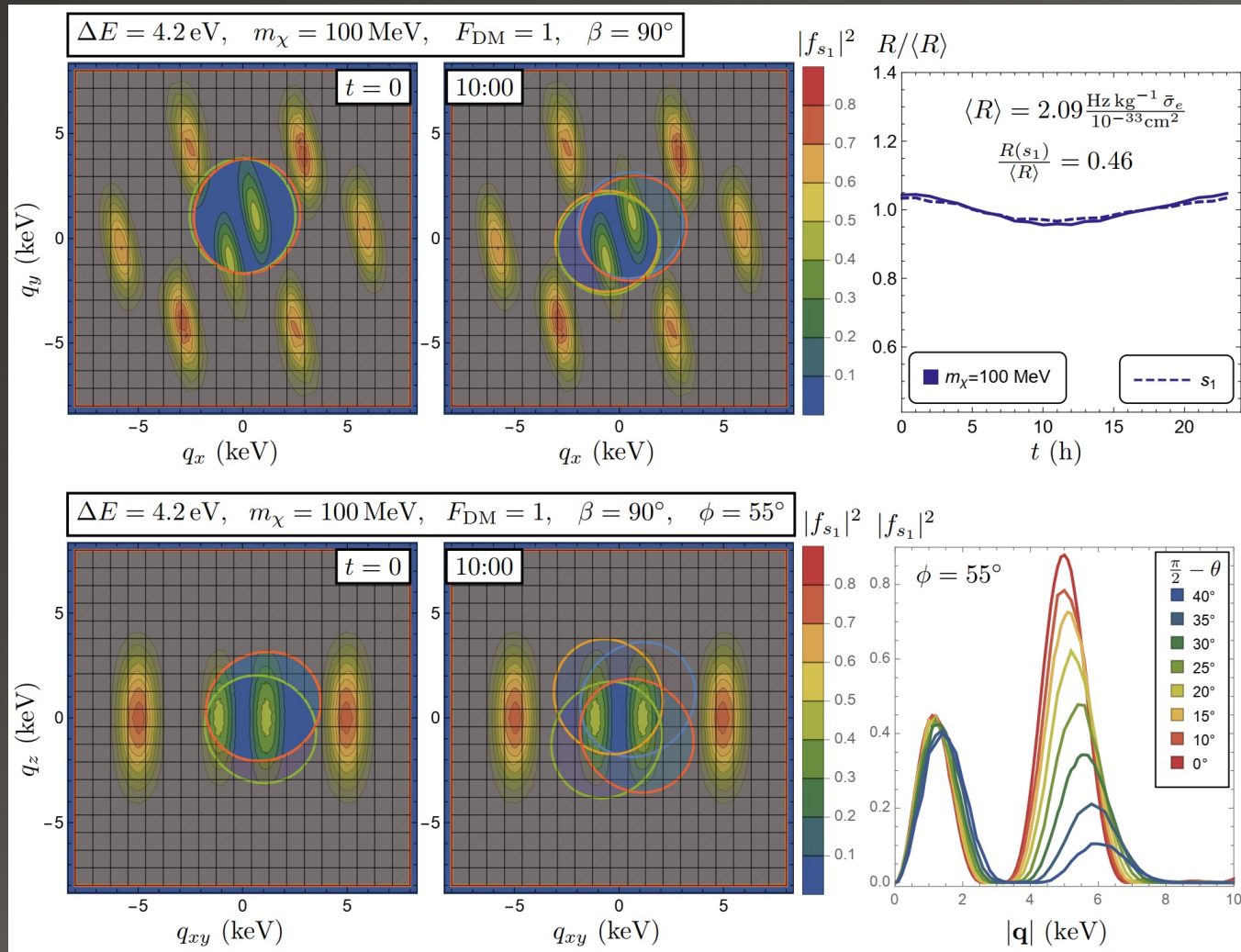
Same as previous figure but for large DM masses, $m_\chi = 100$ MeV. Only the nearly-spherical region near $q \sim 0$ with inner boundary $q_{\min} \simeq 1.6$ keV is kinematically forbidden. As a result, the daily modulation amplitude is smaller, driven by the anisotropy of the inner secondary peaks and the tails of the primary peaks.

QDs – Cheap, tunable and scalable

Φ dependence on the solution concentration for 3nm and 3.3nm PbS QDs in toluene.

$$n_e \sim 10^{20} \text{ cm}^{-3} = 10^{23} \text{ L}^{-1}$$

Strongly Confining Quantum Dots

Semiconducting nano-spheres

$$a << a_0$$

$$E_{\text{confinement}} = \frac{\hbar^2 \pi^2}{2a^2} \left(\frac{1}{m_e} + \frac{1}{m_h} \right) = \frac{\hbar^2 \pi^2}{2\mu a^2}$$

$$E = E_{\text{bandgap}} + E_{\text{confinement}}$$

$$= E_{\text{bandgap}} + \frac{\hbar^2 \pi^2}{2\mu a^2}$$

$$E_{kin} \sim \frac{1}{r^2}$$
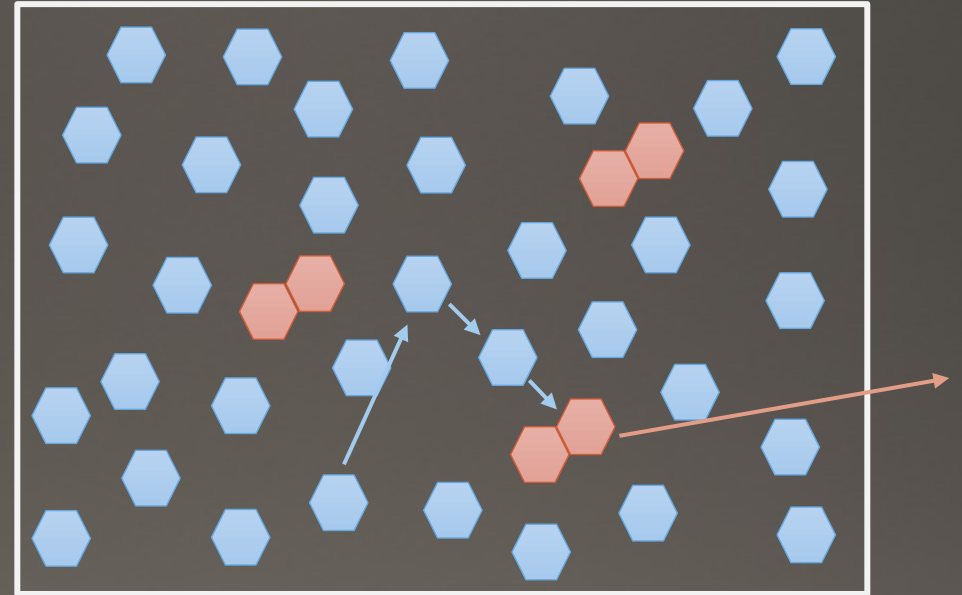
$$E_{coulomb} \sim \frac{1}{r}$$

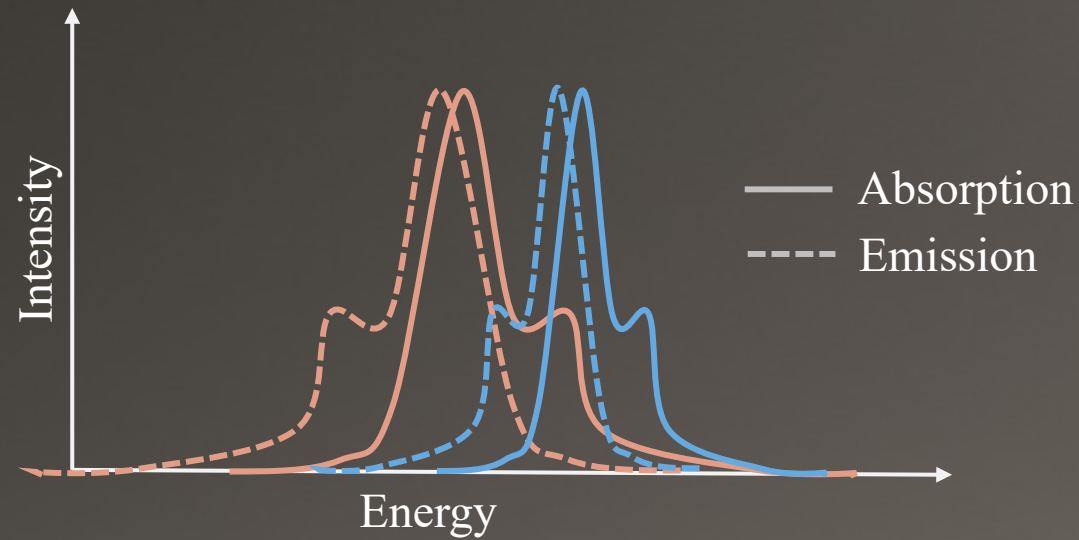# Fluorescence: Binary Scintillators

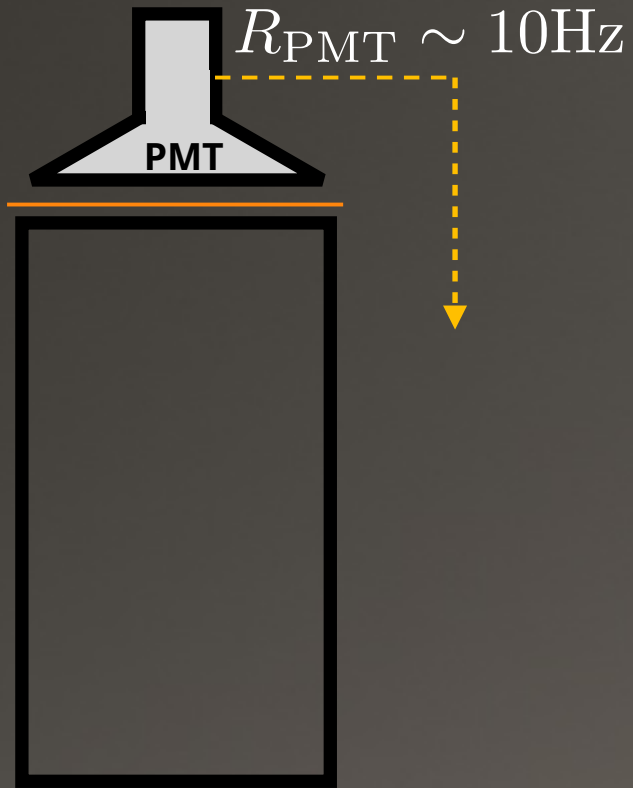Solvent: Primary target starts the signal

Solute: Dilute fluor gets the signal out of the bulk

Intensity

Energy

Absorption
Emission

PbS QDs: Improvements

$R_{\mathrm{PMT}} \sim 10\mathrm{Hz}$

PMT

$R \sim R_{\mathrm{PMT}} + \delta R$

PMT

Target Volume

$R \approx R_{PMT} + \delta R + R_{\gamma-QD}$

$$R_{\gamma-QD} \lesssim \sqrt{R_{\mathrm{PMT}}}$$

"Blind" mode

"Active" mode

PbS QDs: Improvements

$R_{\mathrm{PMT}} \sim 10\mathrm{Hz}$

PMT

$R_{\mathrm{coinc}}^0 \approx \Delta T R_{PMT}^2$

$R \sim R_{\mathrm{PMT}} + \delta R$

PMT
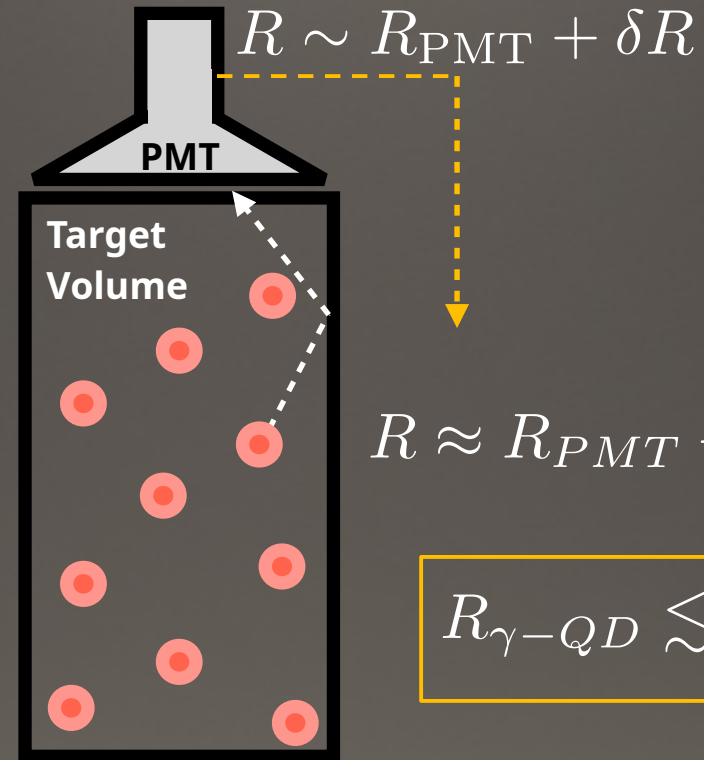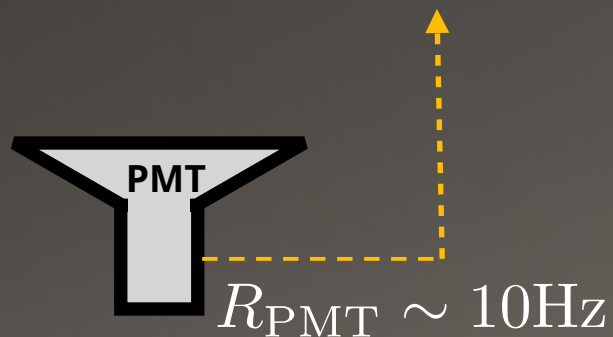
Target Volume
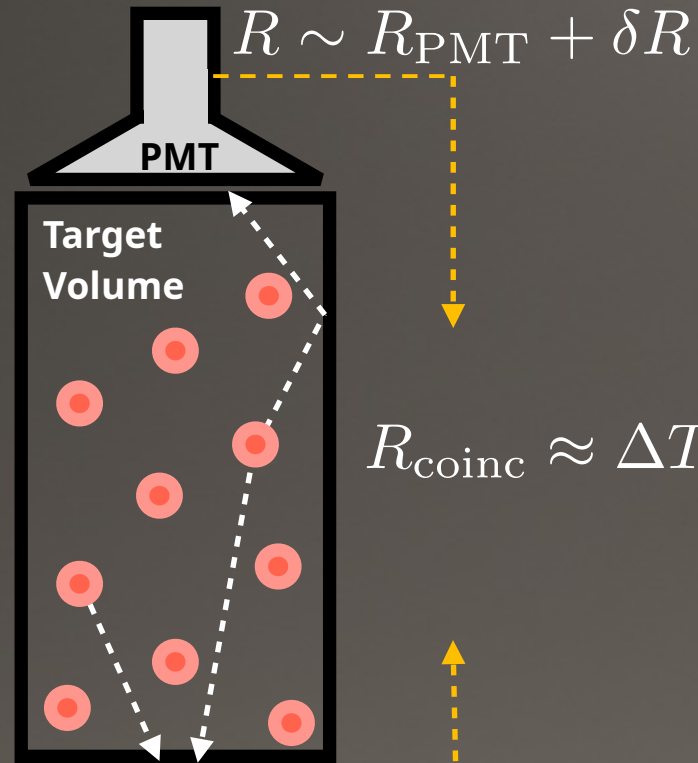
$R_{\mathrm{coinc}} \approx \Delta T R_{PMT}^2 + 2\Delta T R_{\mathrm{PMT}}\delta R + R_{2\gamma-QD}$

$$R_{2\gamma-QD} \lesssim \Delta T R_{PMT}^{3/2}$$

PMT

$R_{\mathrm{PMT}} \sim 10\mathrm{Hz}$

"Blind" mode

PMT

$R \sim R_{\mathrm{PMT}} + \delta R$

"Active" mode

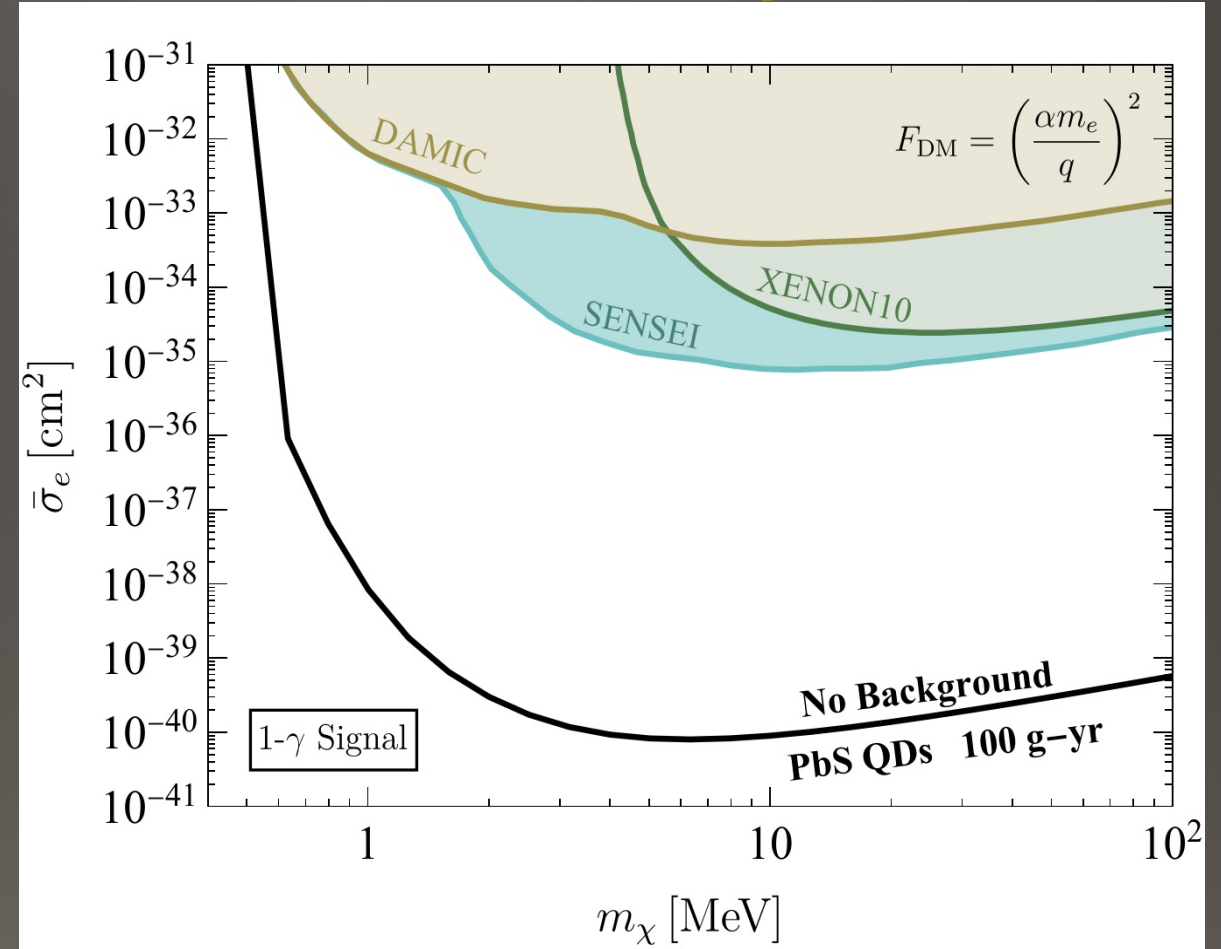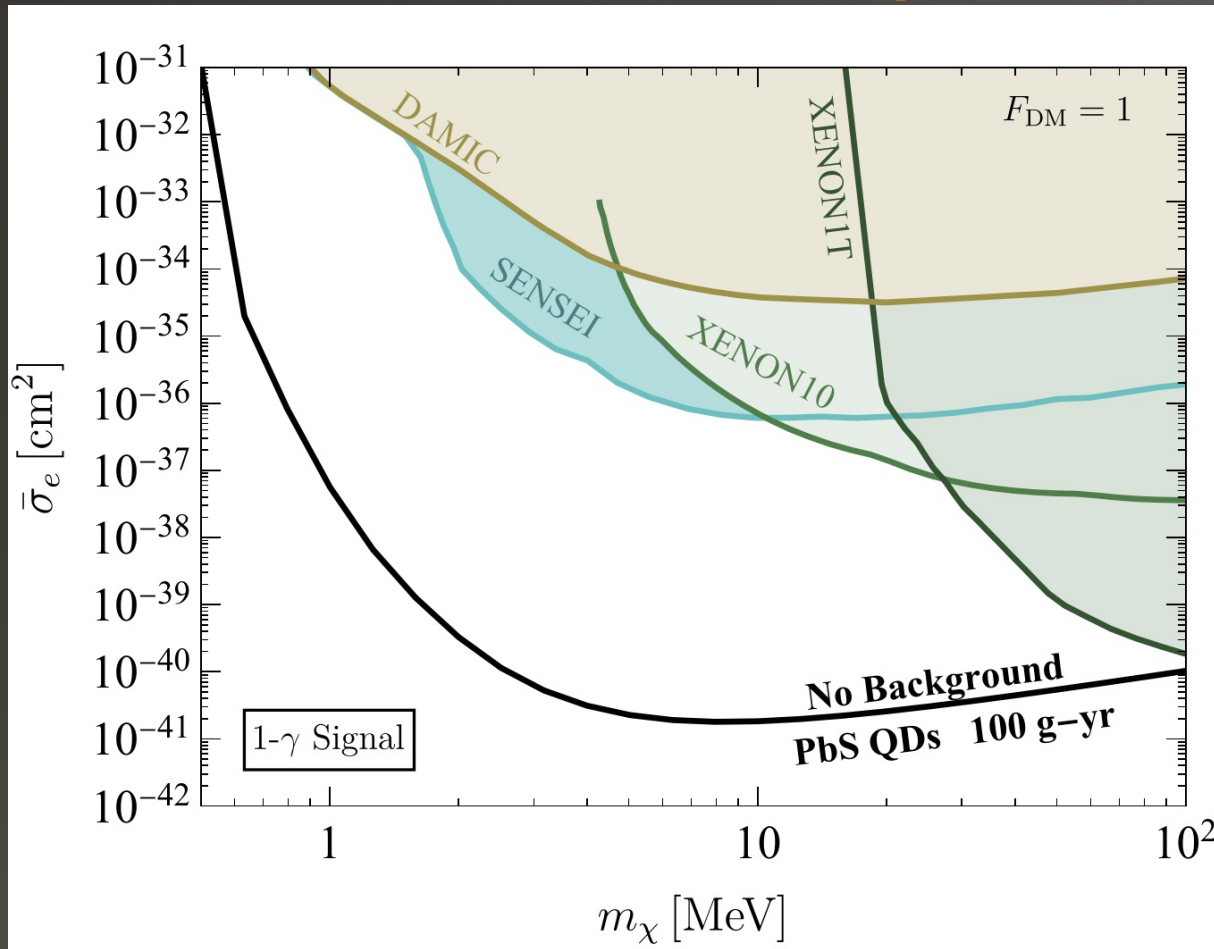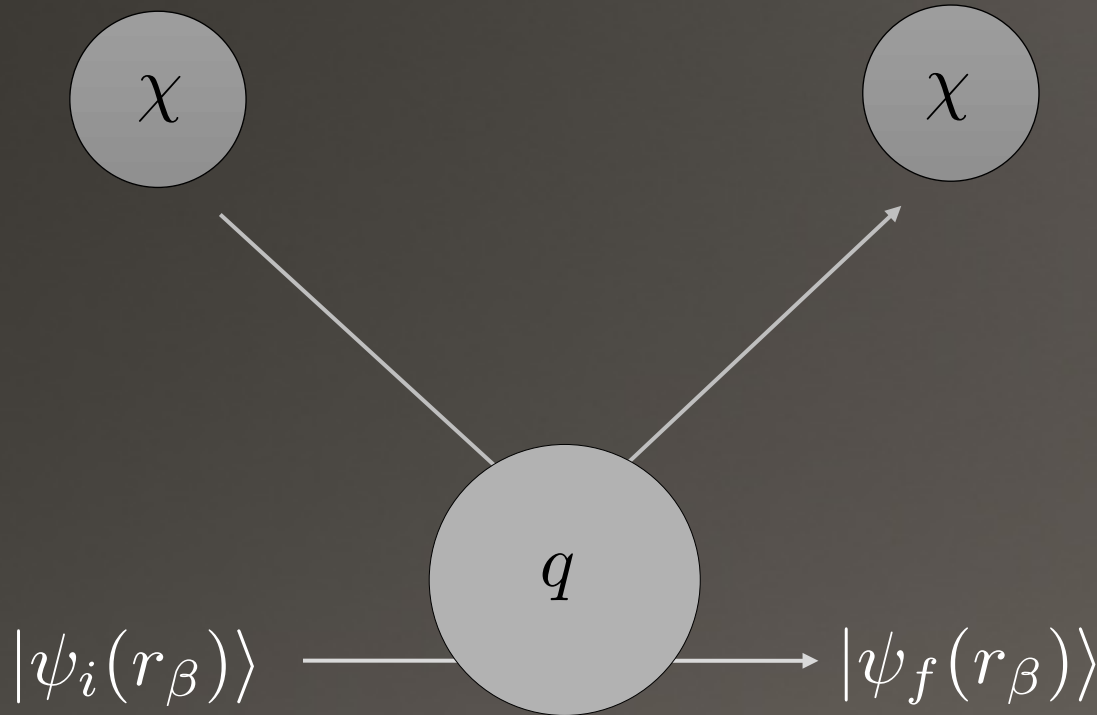# PbS QDs: Optimism for comparison

Blanco '22: 2208.05967

DM-Electron Scattering (no background 1-photon signal)

Electron Recoil: Charge Signal

χ

χ

q

$|\psi_i(r_\beta)\rangle$

$|\psi_f(r_\beta)\rangle$

Electron scattering

$$\Delta E_r = (m_\chi^2/m_{\mathrm{T}}) \times 10^{-6}$$

$$\Delta E \sim \mathcal{O}(\text{few eV}) \left(\frac{m_\chi}{1\,\mathrm{MeV}}\right)^2$$

What has such transition energies?

- Semiconductor band gaps

- Maybe atomic ionization

Electrons in crystals (exciton generation)

$$|\psi_i\rangle \sim u_v(r)e^{ik'\cdot r} \qquad |\psi_f\rangle \sim u_c(r)e^{ik\cdot r}$$

Electrons in atoms (ionization)

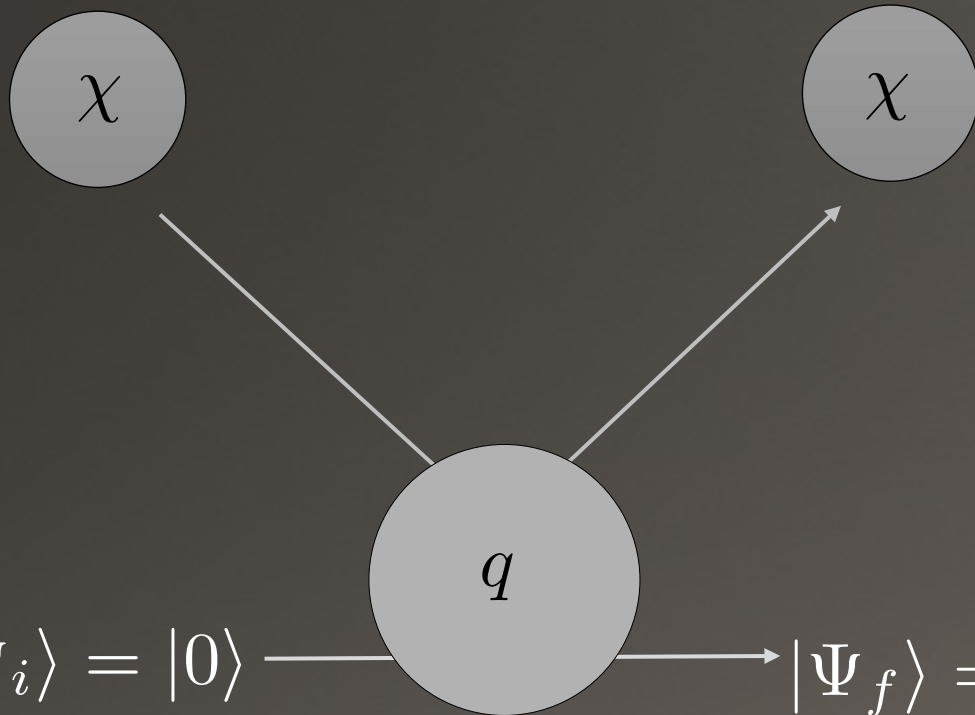$$|\psi_i\rangle \sim \psi_{\mathrm{STO}}(r_\beta) \quad |\psi_f\rangle \sim e^{ik\cdot r}, \, r \gg a_0$$

Semiconductor CCDs
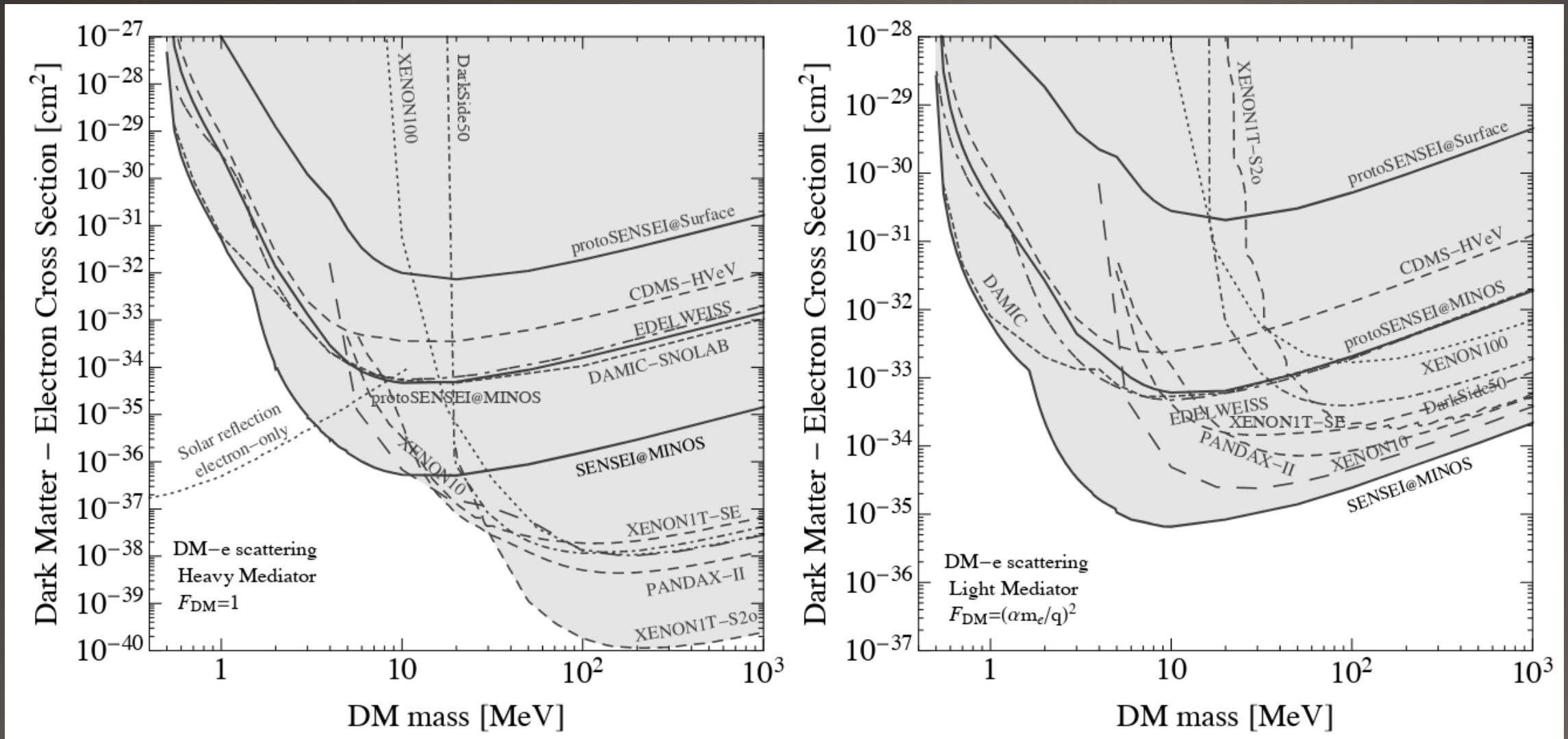
Essig R., et al. "*Snowmass2021 Cosmic Frontier The landscape of low-threshold dark matter direct detection in the next decade*" arXiv:2203.08297 (2022).

Nuclear Recoil: Phonon Signal
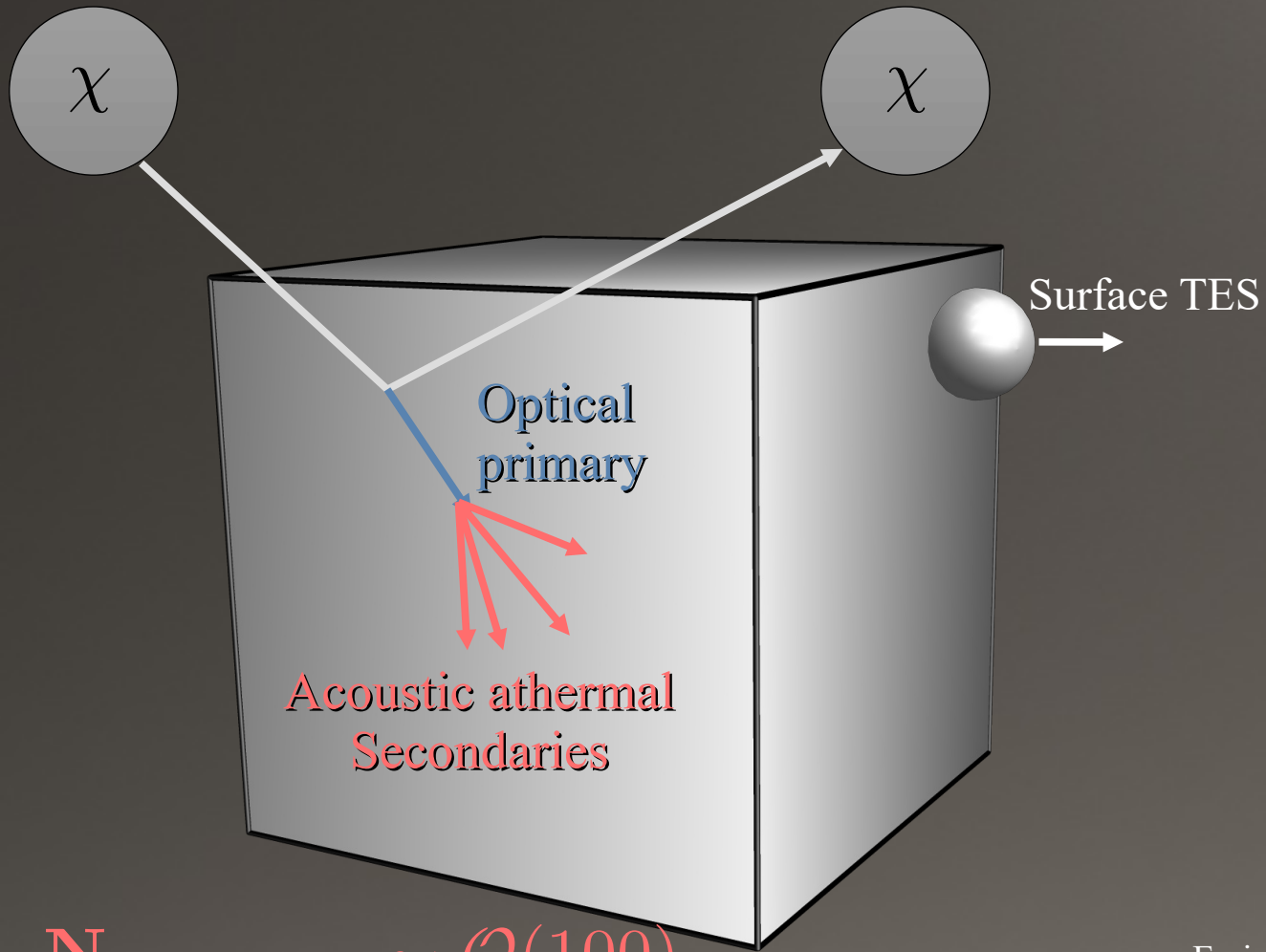
χ

χ

q

Nuclear scattering

$$\Delta E \sim \mathcal{O}(\text{few eV}) \left(\frac{m_\chi}{100\,\text{MeV}} \right)^2 \left(\frac{m_N}{130\,\text{GeV}} \right)^{-1}$$

$$\omega \sim \mathcal{O}(10\text{-}100\ \text{meV})$$

$$|\Psi_i\rangle = |0\rangle \qquad\qquad |\Psi_f\rangle = a^\dagger(k)\,|0\rangle$$

Calorimeters

χ

χ

Surface TES

Optical primary

Acoustic athermal Secondaries

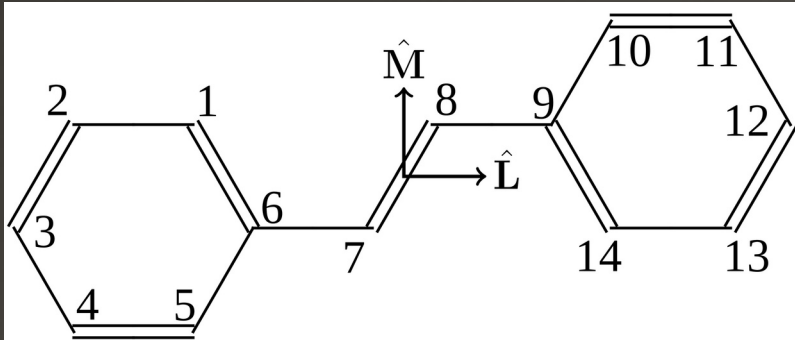$N_{\mathbf{accoustic}} \sim \mathcal{O}(100)$

$E_0 \sim 10 - 100 \text{ meV}$
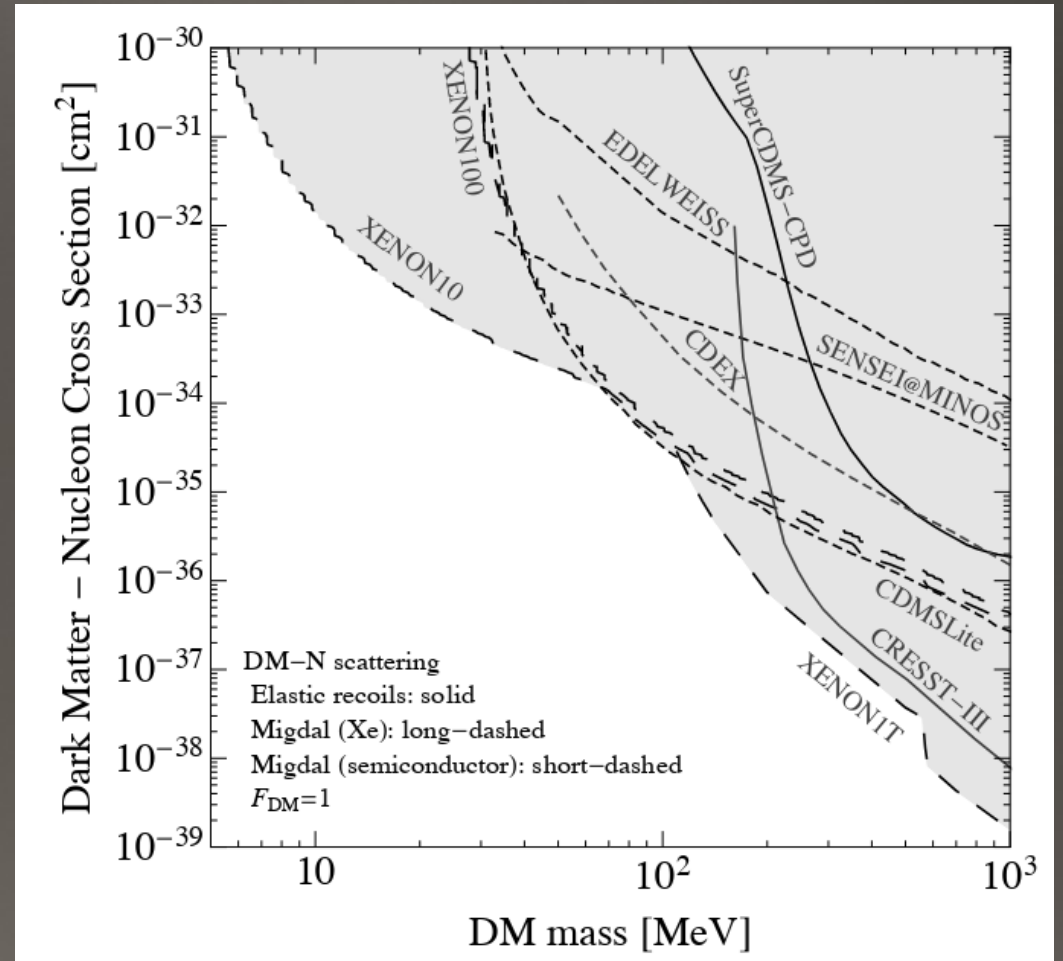
Essig R., et al. *Snowmass2021 Cosmic Frontier The landscape of low-threshold dark matter direct detection in the next decade*" arXiv:2203.08297 (2022).
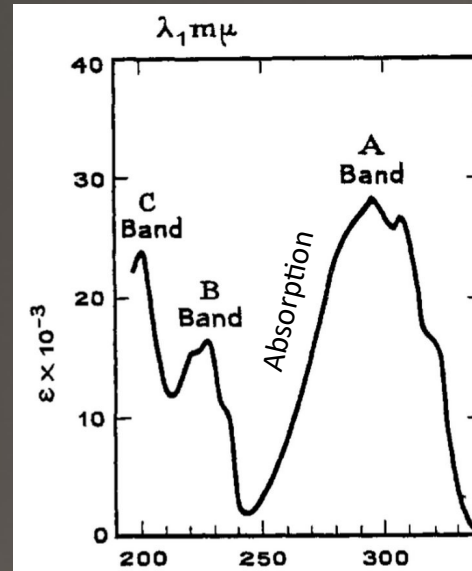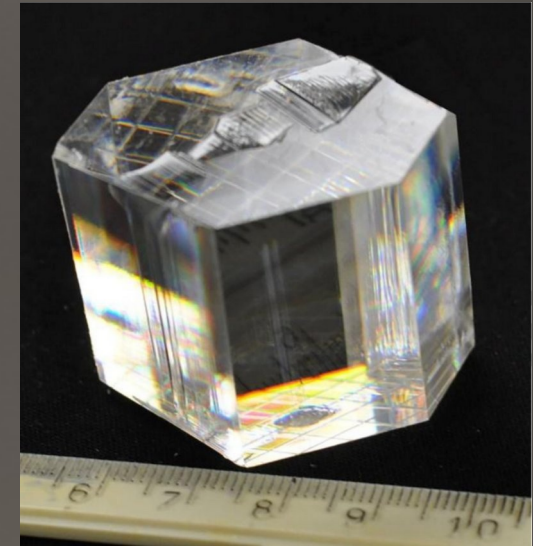
Directional Targets: Polyacenes

Trans-Stilbene

$$E_1 = 4.2\text{eV}$$

Beveridge & Jaffe '65

Dipole allowed E1!

Carman, et.al. '18 (J. of Crystal Growth)

Trans-Stilbene

s	Platt Symbol	Symmetry	ΔE [eV]	Configuration amplitudes			
s_1	^1B	B_u	4.240	$d_{7,8} = 0.94,$	$d_{4,11} = -0.24$		
s_2	$^1G^-$	B_u	4.788	$d_{7,10} = 0.53,$	$d_{5,8} = 0.53,$	$d_{6,11} = 0.37,$	$d_{4,9} = -0.37$
s_3	$^1G^-$	A_g	4.800	$d_{7,9} = 0.53,$	$d_{6,8} = 0.53,$	$d_{5,11} = 0.37,$	$d_{4,10} = -0.37$
s_4	$^1(C,H)^+$	A_g	5.137	$d_{7,11} = 0.41,$	$d_{5,9} = -0.41,$	$d_{6,10} = -0.41,$	$d_{4,8} = -0.59$
s_5	$^1H^+$	B_u	5.791	$d_{5,10} = 0.54,$	$d_{6,9} = 0.54,$	$d_{7,12} = 0.33,$	$d_{3,8} = 0.33$
s_6	$^1G^+$	A_g	6.264	$d_{7,9} = 0.68,$	$d_{6,8} = -0.68$		
s_7	$^1C^-$	A_g	6.013	$d_{7,11} = 0.66,$	$d_{4,8} = 0.54,$		
s_8	$^1G^+$	B_u	6.439	$d_{7,10} = 0.65,$	$d_{5,8} = -0.65$		

Table 1: The first eight excited states $s_{n=1\ldots8}$, with their energy eigenvalues $\Delta E(s_n)$ with respect to the ground state and coefficients $d_{ij}^{(n)}$ as calculated by Ting and McClure.

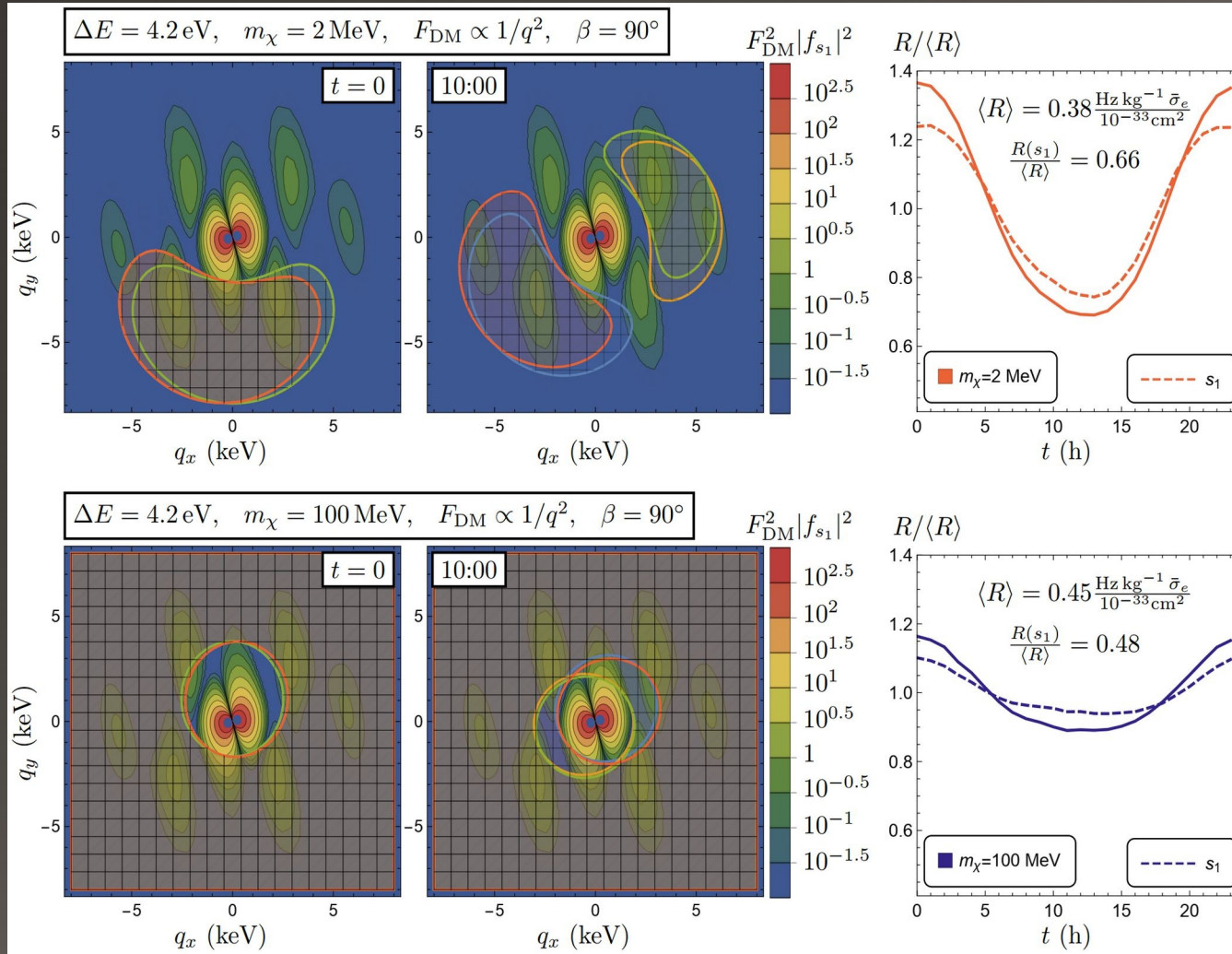$$|s_n\rangle = \sum_{i,j>i} d_{ij}^{(n)} |\psi_i^j\rangle,$$

$$\sum_{ij} |d_{ij}^{(n)}|^2 = 1.$$

$$f_{g\to s_n}(\vec{q}) = \left\langle \psi_{s_n}(\vec{r}_1 \ldots \vec{r}_{14}) \left| \sum_{m=1}^{14} e^{i\vec{q}\cdot\vec{r}_m} \right| \psi_G(\vec{r}_1 \ldots \vec{r}_{14}) \right\rangle$$

$$= \sum_{ij} d_{ij}^{(n)} \left\langle \psi_i^j \left| e^{i\vec{q}\cdot\vec{r}} \right| \psi_G \right\rangle$$

$$= \sqrt{2} \sum_{ij} d_{ij}^{(n)} \langle \Psi_j(\vec{r}) | e^{i\vec{q}\cdot\vec{r}} | \Psi_i(\vec{r}) \rangle.$$

Daily Modulation: Light Mediator

Same as previous figures (top) for a light mediator DM form factor $F_{\mathrm{DM}} = (\alpha m_e/q)^2$. Here, the contour plots show $F_{\mathrm{DM}}^2|f(s_1)|^2$ which appears in the rate integrand; the scattering is dominated by the smallest kinematically-allowed q. **Top:** Molecular form factors with $q_z = 0$ and rate modulations for $m_\chi = 2$ MeV. **Bottom:** Molecular form factors with $q_z = 0$ and rate modulations for $m_\chi = 100$ MeV.

Local DM Phase Space
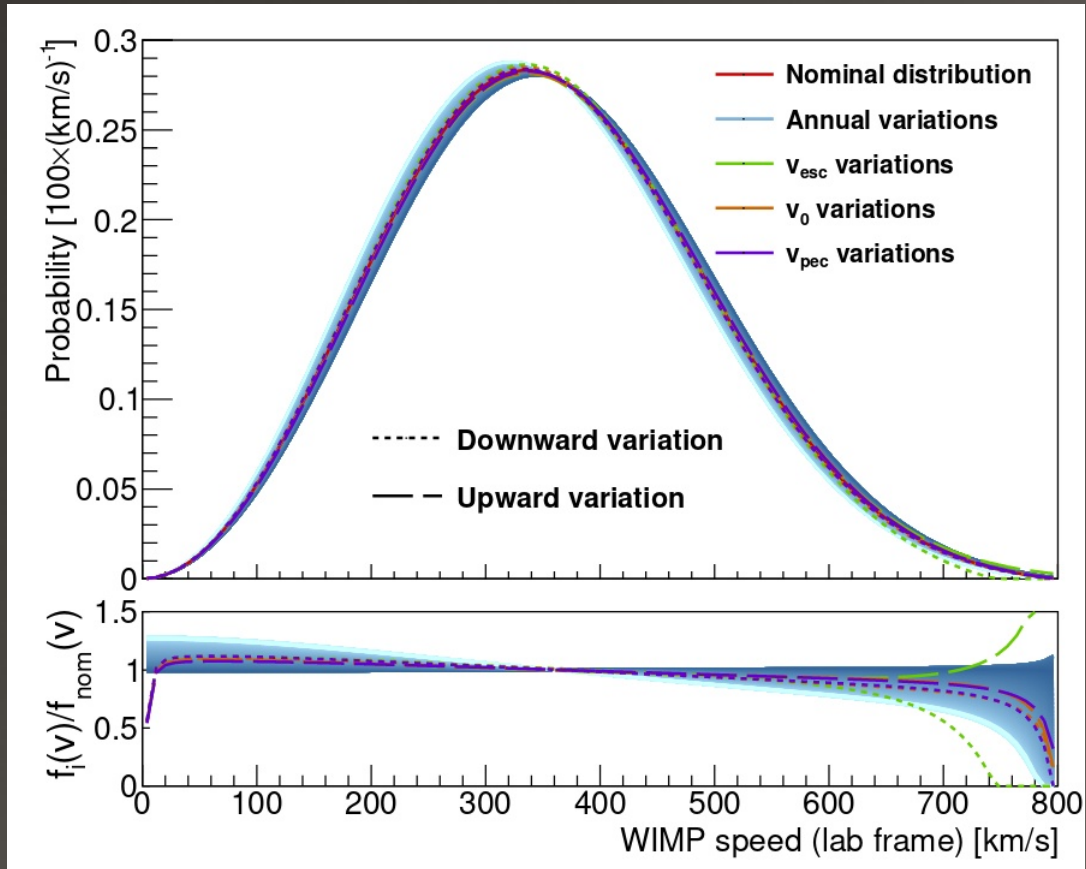
Baxter, D., et al. "*Recommended conventions for reporting results from direct dark matter searches*." The European Physical Journal C 81.10 (2021): 1-19.
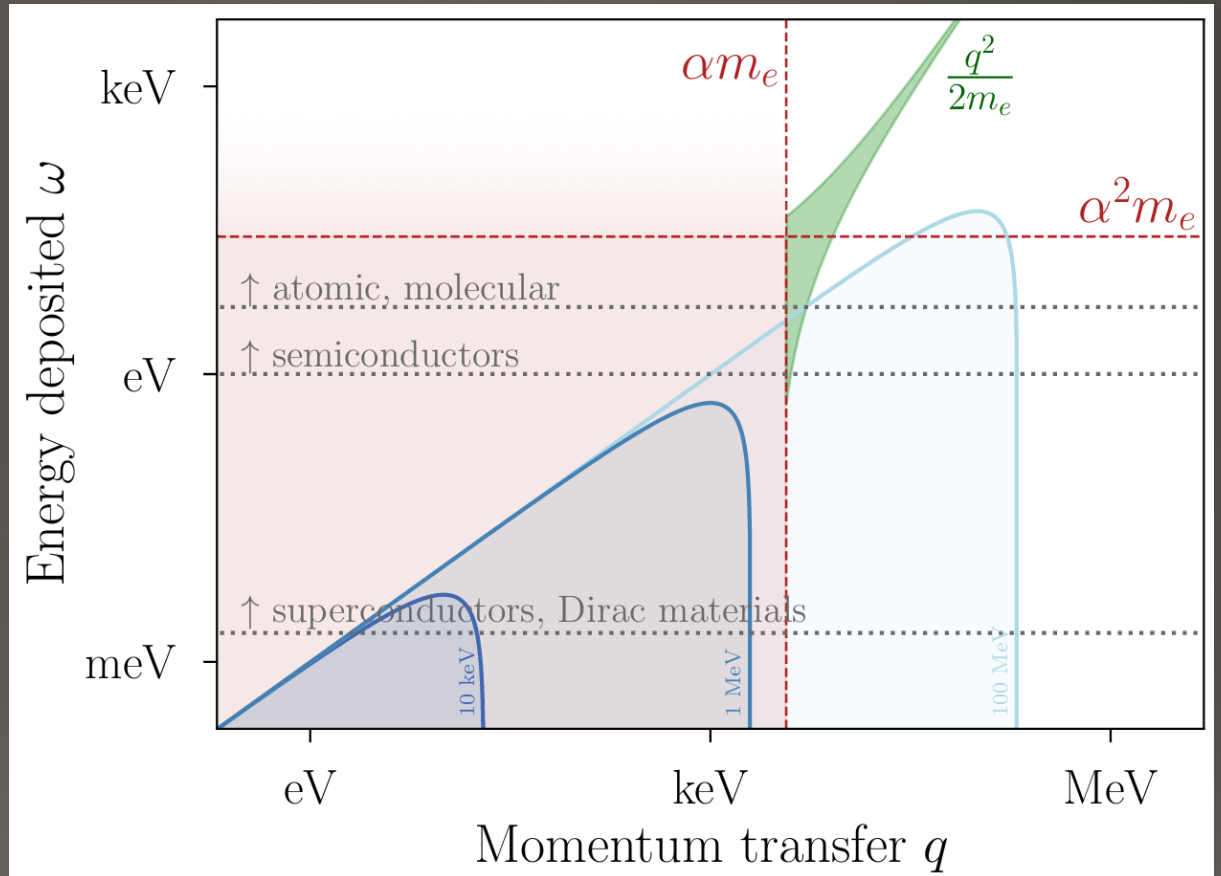
Lin, Tongyan. "*Sub-GeV dark matter models and direct detection*." SciPost Physics Lecture Notes (2022): 043.